ZEUS–13–NNN
5th April 2018

Azimuthal correlations in ep collisions

Jacobus Onderwaater

jonderwaater@gmail.com

GSI

Planckstrasse 1, 64291 Darmstadt

5th April 2018

Abstract

Recent observations at RHIC and the LHC of two- and multi-particle correlations in high multiplicity relativistic proton-proton and proton-ion collisions and similarity of the results to those observed in central heavy-ion collisions are often interpreted as an evidence for collective particle production in small collision systems. These results motivate a study in even smaller systems, such as produced in relativistic electron-proton collisions.

We present a measurement of two-particle correlations in collisions of electron beams at 27.5 GeV with beams of protons at 920 GeV, which corresponds to 318 GeV center-of-mass energy. A sample of events equivalent to the integrated luminosity of 430 pb^{-1} was recorded with the ZEUS experiment in 2003-2007. The correlations are measured for charged hadrons as a function of event multiplicity for the lab pseudo-rapidity range $-1.5 < \eta_{lab} < 2$. To probe the possible contribution due to collective effects, the correlations are studied as a function of the particle's pair separation in pseudo-rapidity and the pair mean transverse momentum. The observed correlations are compared to available Monte Carlo models of deep inelastic electron-proton scattering. Observations based on the analysis of the ZEUS data put a limit on the possible collective effects in high multiplicity e-p collisions.

Contents

1 To do

Trigger vs q2 (should be 1% Event variation (zvertex (compare central to outside 50/50), q2, Siprob, Sitheta, empzPHPcut, empzPHPcutup, elenecut, ntrkcut, trkfraccut, vtxchi2ntrkcut, chimney cut, cal crack cut)
Track variation (efficiency, mc weights, imppar cuts) Period consistency

1.1 Questions

Why is $\eta - vtxz$ distribution not skewed

1.2 Analysis reference (to put in bibliography

Description of data/MC trees: `http://zeusdp.desy.de/ZEUS_ONLY/analysis/comntp/variables/v08/root_variables.html`
Github webpage: `https://gitlab.cern.ch/ISOQUANT/ZEUS`

1.3 to put in appendix

mariellas stuff
move php to appendix
digest presentations for useful info/plots

2 Introduction

commit the code to git

An experimental research program on heavy ion collisions at large collision energy has been performed at RHIC and at the LHC. It was found that many aspects of the particle production at low transverse momentum (up to about 3 GeV) can be described by theoretical models based on relativistic fluid dynamics with thermodynamic information as calculated from QCD (using lattice gauge theory) and with small ratio of shear viscosity to entropy density.

These findings indicate that the dynamical evolution succeeding directly a heavy ion collision can be understood to rather good approximation in terms of a locally thermalized fluid corresponding to a quark-gluon plasma. The theoretical description is in terms of collective fields - more specifically the fluid velocity $u^\mu(x)$, the energy density $\epsilon(x)$, the pressure $p(x)$ related to $\epsilon(x)$ by the thermodynamic equation of state and the shear stress $\pi^{\mu\nu}(x)$ as well as bulk viscous pressure $\pi_{\text{bulk}}(x)$ related to gradients of the fluid velocity by shear and bulk viscosity.

The collective fluid fields are initialized with a reasonable energy distribution and their subsequent dynamics describe a collective expansion, dilution and cool-down. Assuming a transition to hadronic degrees of freedom and a free-streaming phase for temperatures below a certain freeze-out temperature, the fluid dynamic model can describe rather well the transverse momentum spectra of charged and identified particles, as well as different particle correlation functions in the rapidity and transverse directions (see below).

The theoretical description based on fluid dynamics assumes frequent interactions between the constituents of the fluid. These are quarks and gluons at high temperature and hadrons at low temperature. The typical mean free path between collisions must be smaller than the size of the fireball and the mean free time smaller than the expansion time scale. Accordingly, the fluid dynamic description is expected to break down for too small (quasi-) particle densities and for too small extensions of the fireball. It is difficult to make a quantitative statement, however, in particular because interactions are strong at intermediate temperatures in the crossover regime between a hadron gas and the quark-gluon plasma.

The large universality of collective effects found in different collider experiments is certainly a surprise to many physicists in the field and asks for a theoretical explanation. One might hope that this leads to a better understanding of the notoriously difficult soft physics of QCD at small transverse momenta in general, including interesting and important phenomena such as hadronization as a consequence of confinement.

The azimuthal 2-particle correlation is measured for different event multiplicities and differentially (vs $\Delta\eta$, $\langle p_{\mathrm{T}} \rangle$ and Δp_{T}):

$$c'_n = (\Sigma_e w_e (\Sigma_i \Sigma_{j!=i} w_i w_j \cos(n(\varphi_i - \varphi_j)) / \Sigma_{j!=i} w_i w_j)) / \Sigma_e w_e \quad (1)$$

Here Σ_e denotes the loop over events.

In this analysis we focus on the the measurement of two- and four-particle correlations in electron-proton data measured with the ZEUS detector at the HERA collider at DESY in Hamburg.

3 ZEUS detector

Add detector picture and descrispion of relevant detector subsystems including kinematic coverage wrt. to the center of the experiment, angular (polar + phi) coverage, number of layers (maximum number of track points, etc)

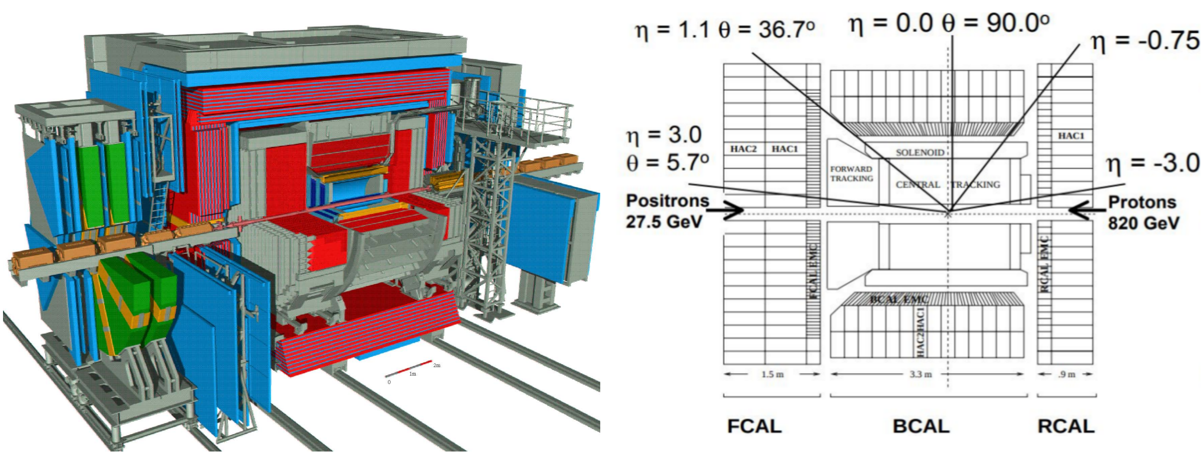

Figure 1: *η, φ, and p_{T} distributions for the various periods.change to one variable per row*

CTD (central tracking) + VTD (vertex traking): $|\eta| < 1.75$ FTD (Forward tracking): $XX < \eta < YY$ Check which detector populates the region of $2 < \eta < 3$ in periods without FTD, check what is the role of TRD detector for tracking

A detailed description of the ZEUS detector can be found elsewhere [?]. A brief outline of the components that are most relevant for this analysis is given below.

In the kinematic range of the analysis, charged particles were tracked in the central tracking detector (CTD) [?] and the microvertex detector (MVD) [?]. These components operated in a magnetic field of 1.43 T provided by a thin superconducting solenoid. The CTD consisted of 72 cylindrical drift-chamber layers, organised in nine superlayers covering the polar-angle[1] region $15^\circ < \theta < 164^\circ$. The MVD silicon tracker consisted of a barrel (BMVD) and a forward (FMVD) section. The BMVD contained three layers and provided polar-angle coverage for tracks from 30° to 150°. The four-layer FMVD extended the polar-angle coverage in the forward region to 7°. After alignment, the single-hit resolution of the MVD was $24\,\mu$m. The transverse distance of closest approach (DCA) of tracks to the nominal vertex in X–Y was measured to have a resolution, averaged over the azimuthal angle, of $(46 \oplus 122/p_T)\,\mu$m, with p_T in GeV. For CTD-MVD tracks that pass through all nine CTD superlayers, the momentum resolution was $\sigma(p_T)/p_T = 0.0029 p_T \oplus 0.0081 \oplus 0.0012/p_T$, with p_T in GeV.

The luminosity was measured using the Bethe-Heitler reaction $ep \to e\gamma p$ by a luminosity detector which consisted of independent lead-scintillator calorimeter [?] and magnetic spectrometer [?] systems. The fractional systematic uncertainty on the measured luminosity was 2.6 %.

4 Analysis method

BEGIN: Analysis steps

1. Apply track-by-track weights extracted from Monte-Carlo (w_i, w_j) multi-differentially as a function of p_T η, charge, separately for different RUN periods (no in-preriod run dependence).
2. No event weights (todo: Test the effect of the electron selection bias)
3. Apply track-by-track weights extracted from data (w_i, w_j) as a function of ϕ, p_T, η, charge, multipicity, and RUN period
4. Calculate the correlation function as a function of
5. Apply the multipicity axis correction: Multiplicity scaled by the efficiency. Add multiplicity correlation plots (true vs. reco) to the AN.

END: Analysis steps

We analyse two- and four-particle correlations:

$$c_n\{2\} = \langle\langle \cos(n(\varphi_\alpha - \varphi_\beta))\rangle\rangle \quad (2)$$

[1] The ZEUS coordinate system is a right-handed Cartesian system, with the Z axis pointing in the nominal proton beam direction, referred to as the "forward direction", and the X axis pointing towards the centre of HERA. The coordinate origin is at the centre of the CTD. The pseudorapidity is defined as $\eta = -\ln\left(\tan\frac{\theta}{2}\right)$, where the polar angle, θ, is measured with respect to the Z axis.

The correlations are calculated using the socalled direct Q-cumulant method for the integrated results (vs particle multiplicity). This employs Q-vectors,

$$Q = \Sigma_j w_j e^{in\varphi_j} \tag{3}$$

where the sum is over particles of interest with azimuthal angle φ in the event. The particles can be weighted with w_j. In this analysis weights are used to correct for tracking efficiency (Sections 7.1 and 7.2). The Q-vectors are used to calculate 2-particle correlations with and without η-gap, and 4-particle correlations without η-gap. The two particle correlations using the same subevent is calculated as follows,

$$c_n\{2\} = (Q_{x,n}^2 + Q_{y,n}^2 - M)/(M(M-1)), \tag{4}$$

and for non-overlapping subevents Q^a and Q^b:

$$c_n\{2\} = (Q_{x,n}^a Q_{x,n}^b + Q_{y,n}^a Q_{y,n}^b)/(M_a M_b). \tag{5}$$

The 4-particle correlation is only calculated with one subevent:

$$\begin{aligned} c_n\{4\} =& (2M(M-3) + (Q_{x,n}^2 + Q_{y,n}^2)^2 - 4(M-2)(Q_{x,n}^2 + Q_{y,n}^2) \\ & - 2Q_{x,n}^2 Q_{x,2n} + 2Q_{x,n}Q_{y,n}Q_{y,2n} - Q_{y,n}^2 Q_{x,2n} \\ & + Q_{x,2n}^2 + Q_{y,2n}^2)/(M(M-1)(M-2)(M-3)). \end{aligned} \tag{6}$$

The 2-particle calculation is also measured differentially (vs $\Delta\eta$, $\langle p_\mathrm{T}\rangle$ and Δp_T). In these cases a nested loop is used:

$$c'_n = (\Sigma_e w_e (\Sigma_i \Sigma_{j!=i} w_i w_j \cos(n(\varphi_i - \varphi_j))/\Sigma_{j!=i} w_i w_j))/\Sigma_e w_e \tag{7}$$

Here Σ_e denotes the loop over events. The event weight w_e used is $M(M-1)$, where M is the event multiplicity. Since we calculate observable is in unit bins of multiplicity, the weight is not relevant.

The statistical error is calculated as in `https://raw.githubusercontent.com/alisw/AliPhysics/vAN-20170625/PWG/FLOW/Base/AliFlowAnalysisWithQCumulants.cxx` line 14260. This contains the following components:

$$
\begin{aligned}
\text{spread} &= \sqrt{\frac{\Sigma_i c_i^2 w_i}{\Sigma_i w_i} - (\frac{\Sigma_i c_i}{\Sigma_i w_i})^2} \\
\text{termA} &= \frac{\sqrt{\Sigma_i w_i^2}}{\Sigma_i w_i} \\
\text{termB} &= \frac{1}{\sqrt{1 - \text{termA}^2}} \\
\text{statistical error} &= \text{spread} * \text{termA} * \text{termB}
\end{aligned} \tag{8}
$$

Here c_i is the measured correlation in an event and w_i the event weight.

5 Data & MC samples and trigger, event & track selection

The measurement is based on data collected with the ZEUS detector at the HERA collider during the period 2003–2007 where an electron beam of energy 27.5 GeV collided with a proton beam of 920 GeV. The integrated luminosity was 430 pb^1 for ep centre-of-mass energies of 318 GeV.

5.1 Data samples

Dataset	Version	All events	GEN	PHP	DIS
03p	v08b	3.705.503	0	314.602	241.032
04p	v08b	47.469.782	0	0	0
05e	v08b	132.155.627	0	16.774.131	16.745.428
06e	v08b	44.169.099	0	0	8.800.000
06p	v08b	86.625.931	0	11.305.261	11.811.492
07p	v08b	41.164.138	0	5.047.470	5.402.077

Table 1: *The analyzed data samples and number of events passing corresponding trigger cuts.*

Calculate total statistics after all cuts, - before and after multi-trigger threshold cut

Update the table for 06e period, discard 03p (low statistics), and use as areference for QA ratios the 05e

5.2 MC samples

Add section with a table for Monte-Carlo description

5.3 Trigger selection

Produce ALL QA plots consistently throughout the AN after event selection and kinematic cuts (except of kinematic variables itself All mentioned variables should also be human readable

The data was recorded with several triggers, which can be grouped and classified as the photoproduction (PHP) and deep inelastic scattering (DIS) triggers.

5.3.1 Deep inelastic scattering (DIS)

DIS:
Trigger bit:
distltfired

Sinistra candidate:
orange.Sincand > 0

Sinistra energy, probability and θ:
$q^2(orange.Siq2el[0]) > 5$
electron candidate probability $(orange.Siprob[0]) > 0.9$
electron $\theta(orange.Sith[0]) > 1.)$

$E - p_z$ within range, and with electron energy above: (define what exactly is E and p_z)
$47 < E - p_z < 69$ GeV, $E_e > 10$ GeV.

In addition there are number of regions of the detector coverage excluded:

```
Veto DIS if following in the folowing cases.

chimney cut (RCAL):
if ( (Sipos[0][0] > -10) && (Sipos[0][0] < 10   )  &&
     (Sipos[0][1] > 110) && (Sipos[0][2] < -141.))

radius cut:
```

```
sqrt( TMath::Power((Sipos[0][0] + 1),2.0) + TMath::Power(Sipos[0][1],2.0) ) < 15)

HES fiducal/CAL crack cut (RCAL)
if ( ( (    (Sipos[0][0] > 5) && (Sipos[0][0] < 11) && (Sipos[0][1] > 0.)   )
          || ( (Sipos[0][0] > -15) && (Sipos[0][0] < -9) && (Sipos[0][1] < 0.) ) )
    && ( Sipos[0][2] < -141.) )

require at least 3 CTD superlayers
should change this to "or" with at least one MVD hit!
should allow +z satellite peak!
cut on energy/momentum consistency
if ( (Sinrsl[0] < 3) || (Sitrkp[0] < 0.3 * Sicalene[0]) || (run < 45000))
```

5.3.2 Photoproduction (PHP)

Trigger requirement on 2 jets > 4.5 GeV.

5.4 Event selection

Event quality selection:

- $-30 < vtxz < 30$ cm Add distributions for Multiplcity:vertex, and rapidity distribution vs vertex for multiplicity above trigger threshold
- Fraction of tracks associated to event vertex > 0.1
- N_{vtx}tracks> 0
- Event vertex wrt beam spot $(vtx_{xy}) < 0.5$
- *Event vertex* χ^2*/tracks associated to vertex* < 50

5.5 Track selection

We select particles in the kinematic range of:

- $0.1 < p_{\mathrm{T}} < 5$ GeV$/c$
- $-1.5 < \eta < 2.0$
- Tracks constrained to the vertex (orange.Trk_prim_vtx = true) (check exact defintion of this variable)

- Exclude scattered electron (orange.Trk_id[itrack] $\neq$ orange.Sitrknr[0]) (check if the electron is im the kinematic range of our selection)
- Impact parameter $DCA_{xy} < 1.0$ cm (check exact defintion of this variable)
- List the track quality variables and add QA of those to the AN (e.g. number of hits CTD (central tracking) + VTD (vertex traking))
- check if there are electrons in the track sample and what is the fraction of it for different charges (positive - negative)

6 Data QA and comparisions with MC

6.1 Trigger

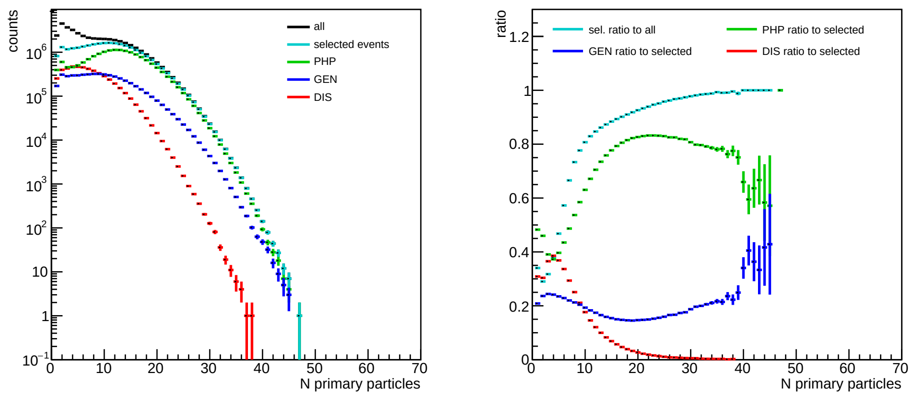

Figure 2: *Trigger selections*

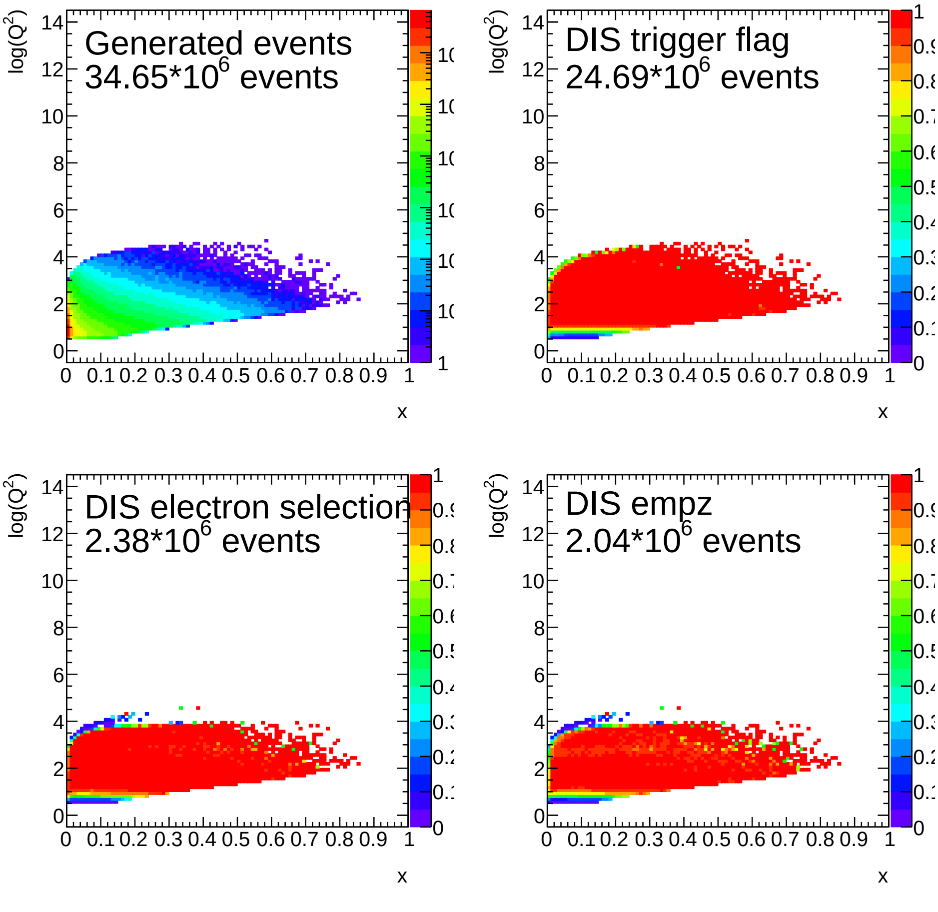

Figure 3: *Trigger electron q2 vs x*

The following figures show the distributions for the trigger selection.

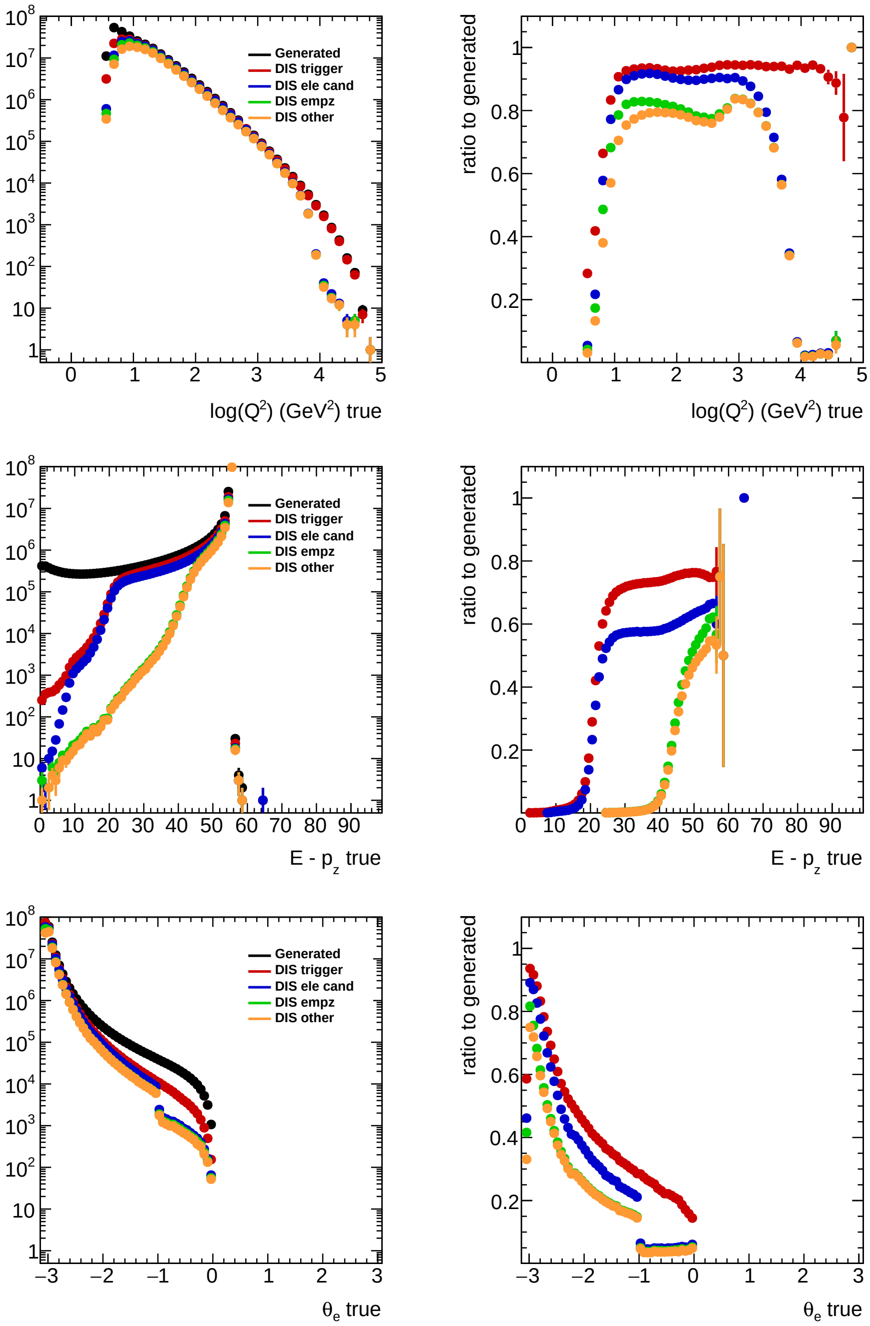

Figure 4: *Effect of DIS electron selections using all events from ari_incl_nc_DIS_lowQ2. The distribution are true values: Mc_q2, Mc_esum-Mc_ez and θ as calculated from momentum components.*

The legend refers to "Generated" for all events in the Monte Carlo sample, "DIS trigger" for the DIS trigger flag being true, "DIS ele cand" for the electron properties $\theta_e > 1.0$, $P_e > 0.9$ and $Sinq2el[0] > 5.0$, "DIS empz" for $47 <$ `V_h_e_zu- V_h_pz_zu` < 69 and $E_e > 10$ GeV. "DIS other" refers to a number of detector cuts as listed in Section 5.3.1.

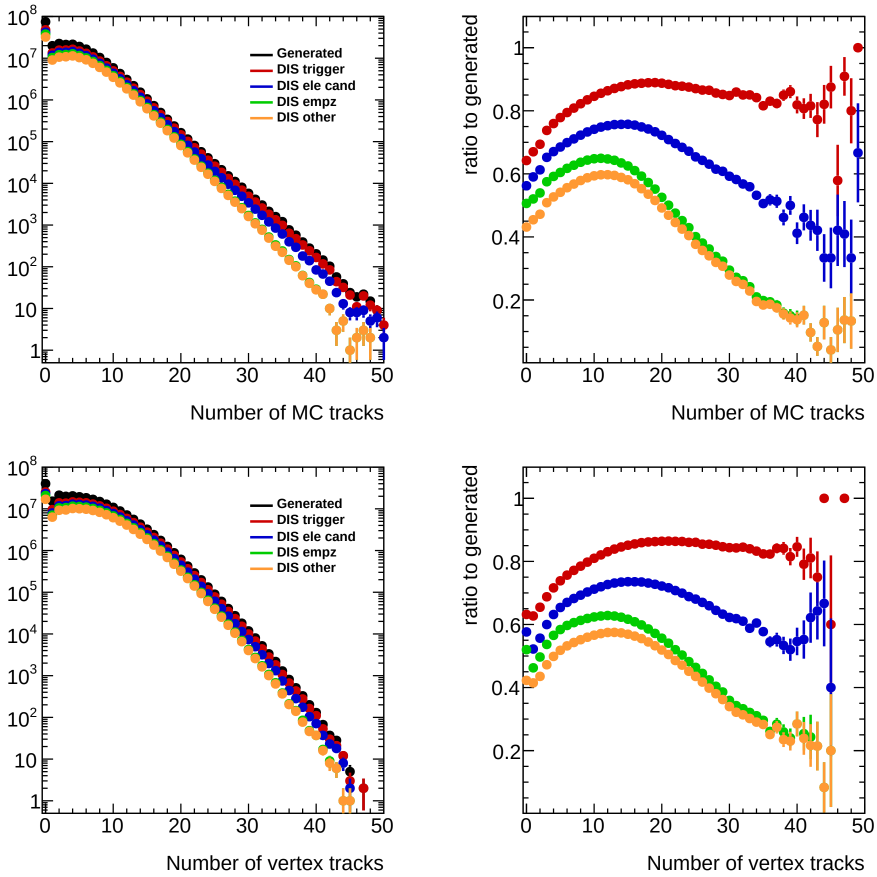

Figure 5: *Effect of DIS electron selections on multiplicity distributions using all events from ari_incl_nc_DIS_lowQ2. Top: distribution of the number of selected primary MC particles. Bottom: distribution if the number of vertex tracks.*

The following figures show the distributions for the trigger selection. In this case "Generated" refers to Monte Carlo events where DIS selection is applied to MC truth parameters: Mc_q2, Mc_Ele_Theta, Mc_Ele_E, empz (Mc_esum-Mc_ez):

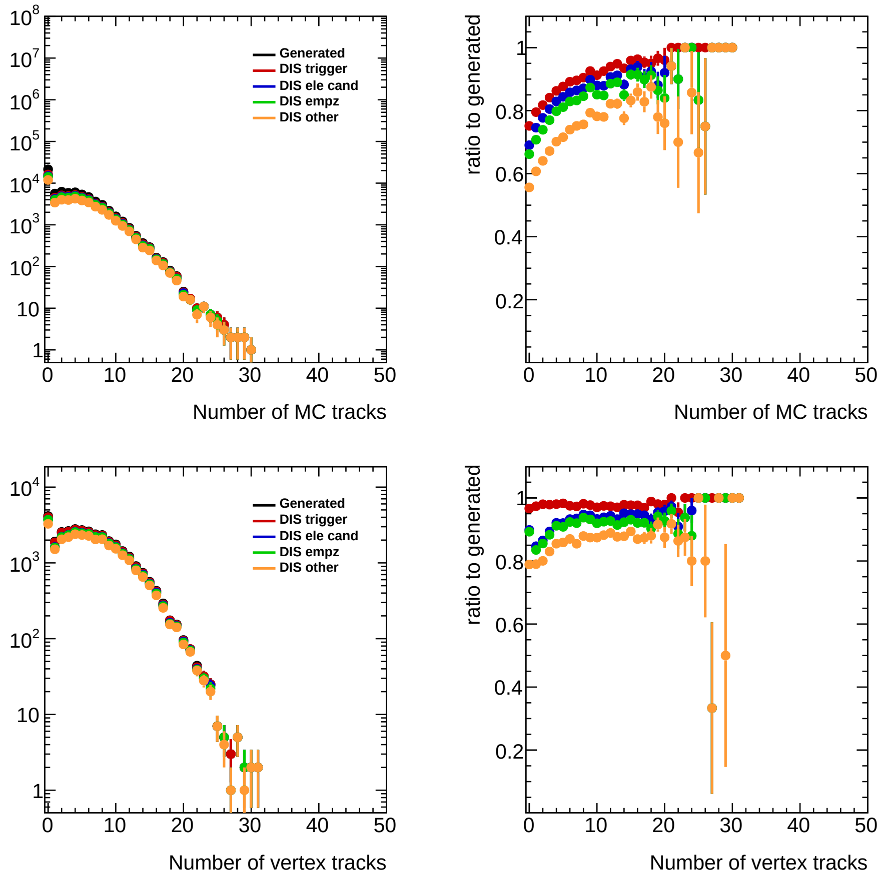

Figure 6: *Effect of DIS electron selections on multiplicity distributions using MC truth selected DIS events from ari_incl_nc_DIS_lowQ2. Top: Mc_q2* $> 5\ GeV^2$. *Bottom: Mc_q2* $> 10\ GeV^2$.

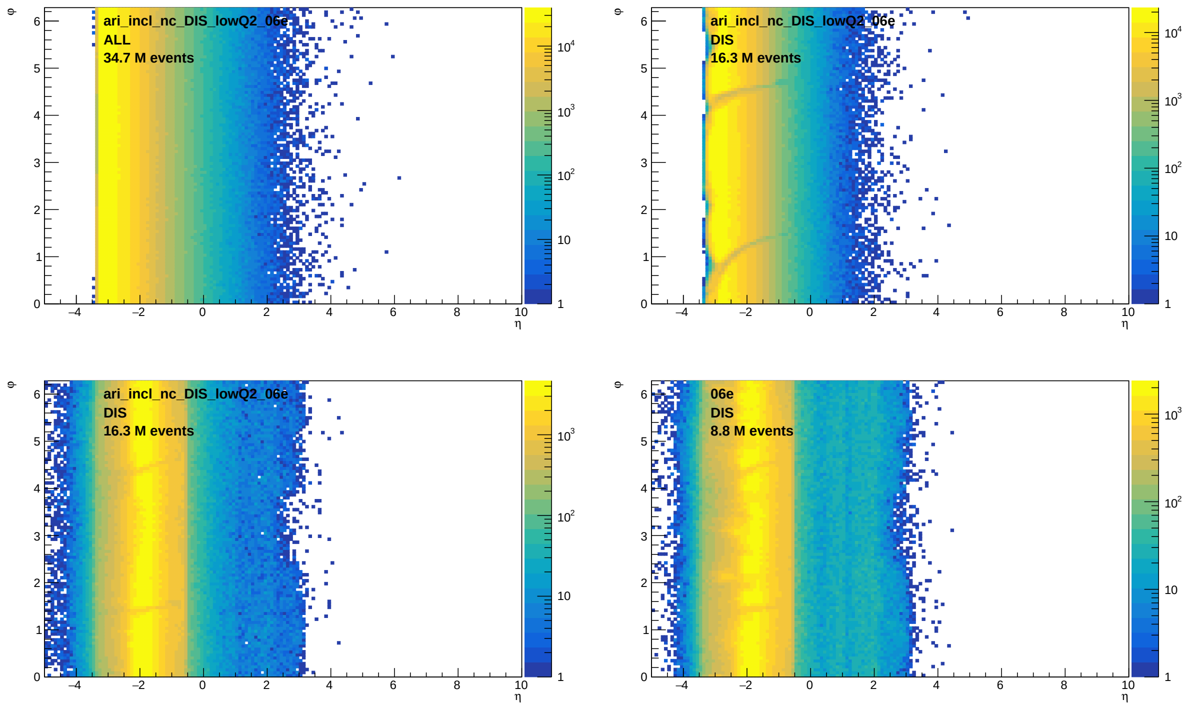

Figure 7: *Top left: MC scattered electron from all generated events (true level). Top right: MC scattered electron passing all DIS selections (true ele). Bottom left: MC scattered electron passing all DIS selections (reco ele). Bottom right: DATA scattered electron passing all DIS selections.*

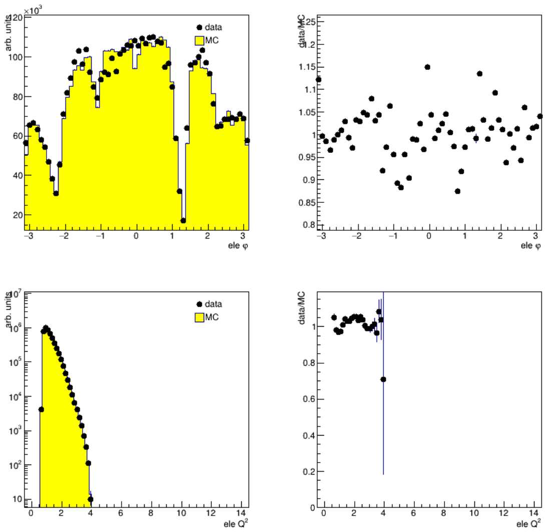

Figure 8: *Electron distributions of data and MC. The distributions are for DIS selected events from 06p and ari_incl_nc_DIS_lowQ2_06e. In the first and third column the distribution in MC (yellow) and data (black dots), with to the right of that the ratios of data to MC.*

273 ## 6.2 Events

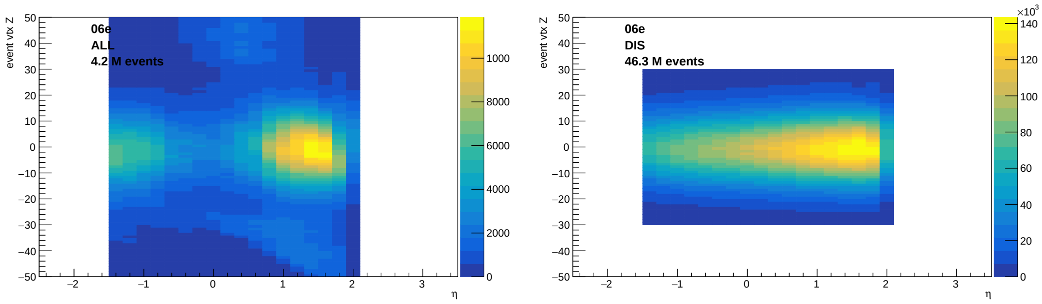

Figure 9: *Event vertex Z vs track η. Left: before quality selection. Right: after quality selection add units*

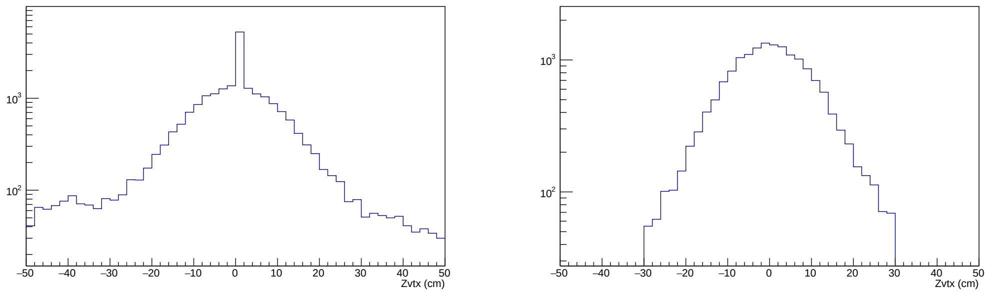

Figure 10: *Event vertex Z. Left: before quality selection. Right: after quality selection*

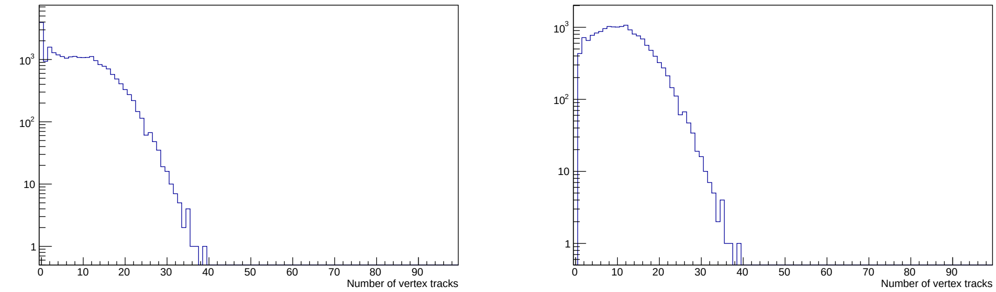

Figure 11: *Number of vertex tracks. Left: before quality selection. Right: after quality selection*

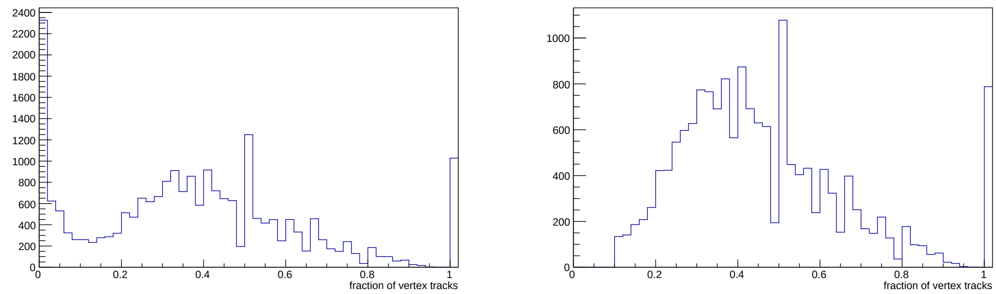

Figure 12: *Fraction of vertex tracks. Left: before quality selection. Right: after quality selection*

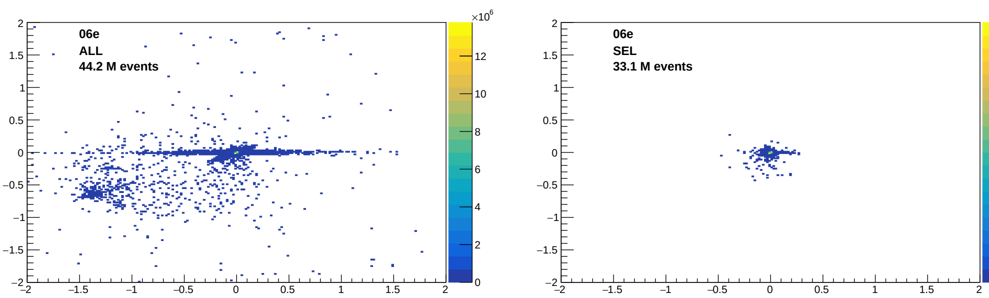

Figure 13: *Left: before quality selection. Right: after quality selection*

To gain some confidence that the data is accurately described by the MC we compare different event and track distributions.

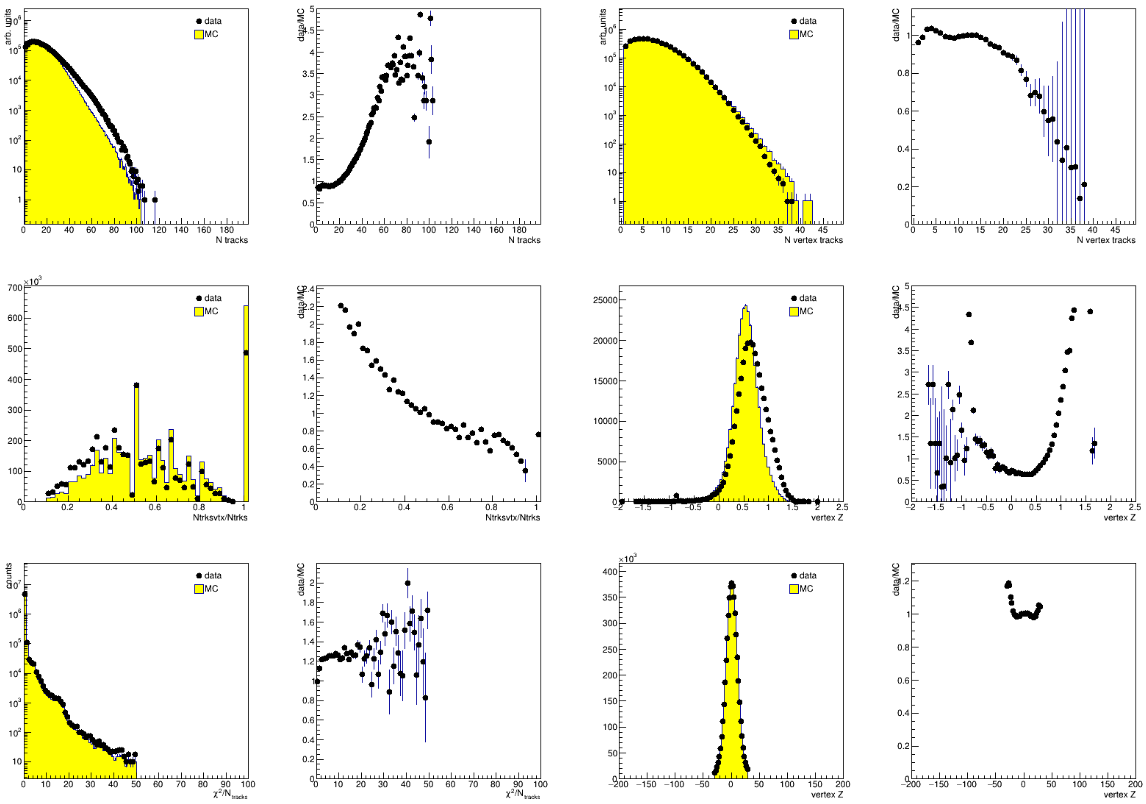

Figure 14: *Event distributions of data and MC. The distributions are for DIS selected events from 06p and ari_incl_nc_DIS_lowQ2_06e. In the first and third column the distribution in MC (yellow) and data (black dots), with to the right of that the ratios of data to MC.*

6.3 Tracks

- Add distribution for these variables beforea nd after the cuts
- Add distribution for 2D x vs. y and projection on a log scale (to see that we do not have junk passed the cuts)
- Are there any vertex quality cuts?
- Multiplicity distribution for different periods
- Add distributions of DIS event selection and relevant QA
- Add matrix for efficiency of DIS selection vs. Q2, multiplicity, rapidity, phi and pT of the electron
- Add 2d q2 truth vs q2 reco
- Add for tracks (phi truth - phi reco) vs pt
- Add Siprob, Sitheta
- Add multiplicity selected tracks vs multiplicity all tracks and vertex tracks vs all tracks
- Add multiplicity selected tracks vs calorimeter energy
- Add 2d beamspot

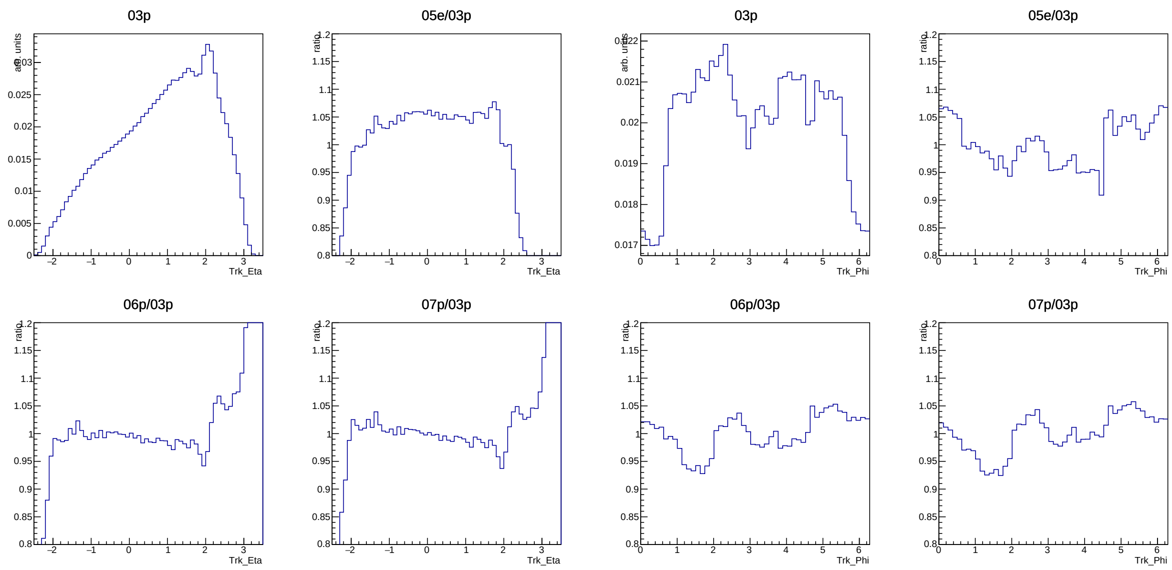

Figure 15: *η, φ, and p_{T} distributions for the various periods.change to one variable per row*

[h]

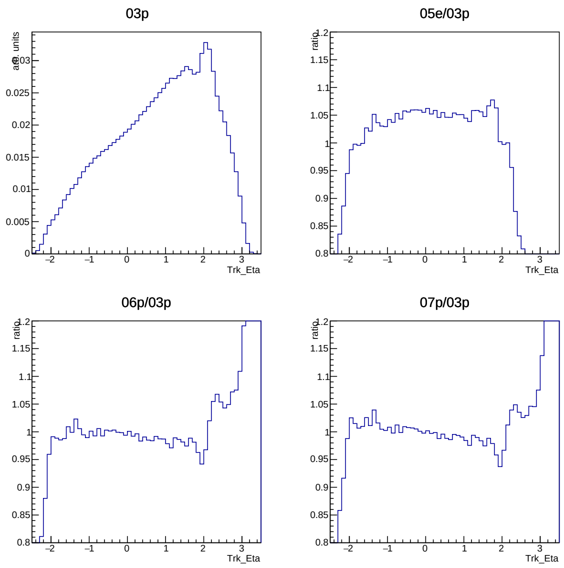

Figure 16: *$\eta - \varphi$ distribution for the various periods.* *add proper figures*

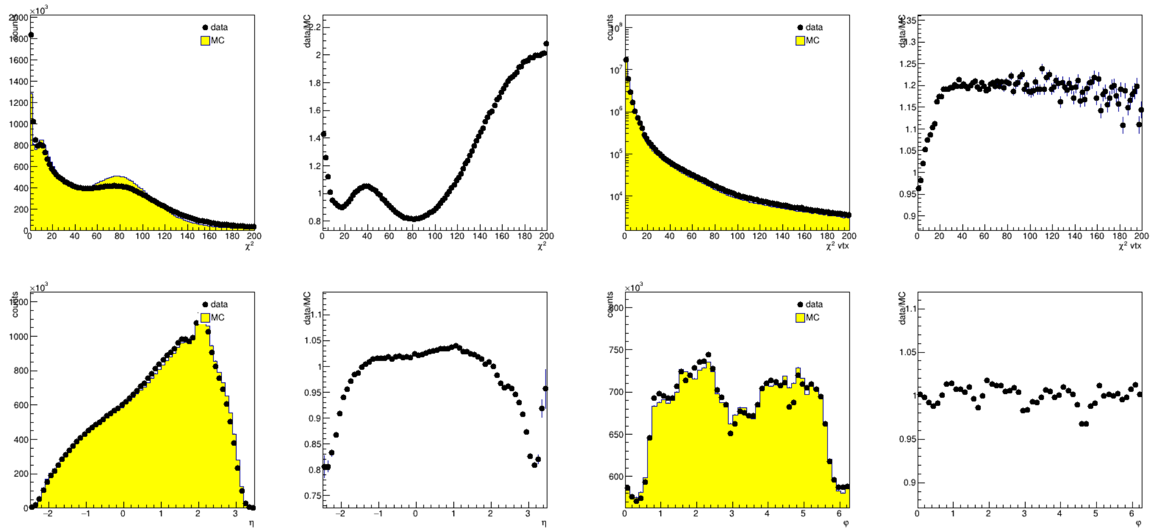

Figure 17: *Track distributions of data and MC. The distributions are for DIS selected events from 06p and ari_incl_nc_DIS_lowQ2_06p. In the first and third column the distribution in MC (yellow) and data (black dots), with to the right of that the ratios of data to MC.*

7 Corrections

We use MC to estimate the tracking efficiency.

7.1 Determining tracking efficiency

The tracking efficiency is estimated by comparing generated charged primary tracks to tracks that are reconstructed as primary particles. Our primary particles are determined as follows from truth: all charged particles with a lifetime longer than $\tau = 1 fm/c$, that are produced within 1 cm of the event vertex, excluding the scattered electron. All reconstructed charged tracks in the orange tree that pass the track selection are considered primary, excluding the scattered electron. The tracking efficiency is calculated in slices track pseudorapidity, track charge and for each period separately.

Specie	Width Γ (GeV)	Mean proper lifetime τ (ps)	(cm/c)
p^+	0	∞	∞
γ	0	∞	∞
K^0	0	∞	∞
e^-	0	∞	∞
n	7.478×10^{-28}	$8.861 \times 10^{+14}$	$2.656 \times 10^{+13}$
μ^-	2.996×10^{-19}	$2.212 \times 10^{+06}$	$6.63 \times 10^{+04}$
K^0_L	1.287×10^{-17}	$5.148 \times 10^{+04}$	1543
π^+	2.528×10^{-17}	$2.621 \times 10^{+04}$	785.7
K^+	5.317×10^{-17}	$1.246 \times 10^{+04}$	373.6
Ξ^0	2.27×10^{-15}	291.9	8.751
Λ	2.501×10^{-15}	264.9	7.943
Ξ^-	4.02×10^{-15}	164.8	4.941
Σ^-	4.45×10^{-15}	148.9	4.464
K^0_S	7.351×10^{-15}	90.14	2.702
Ω^-	8.071×10^{-15}	82.1	2.461
Σ^+	8.209×10^{-15}	80.72	2.42

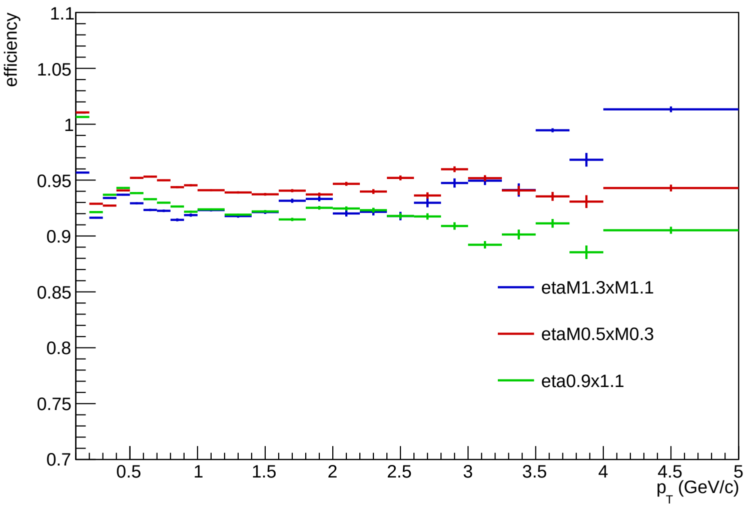

Figure 18: *Left: primary particles. Right: Track efficiency determined for positive tracks in ari_incl_nc_DIS_lowQ2_06p.*

7.2 Non-uniform corrections

The corrections for non-uniformity are done by applying φ-weights in bins of η, particle charge and event multiplicity. First the uncorrected φ-distributions are obtained with a pass over the data, while considering the p_{T}, η-weights. Then the φ-weights are calculated by assuming that the distributions should be uniform, while maintaining the total yield per η, charge and event multiplicity slice. An example of weights is shown in Figure 19.

The φ-weights should not change the integral, since that is set by the p_{T}, η-weights extracted from MC. The effect of the φ weights on the η-distribution is shown in Figure 20.

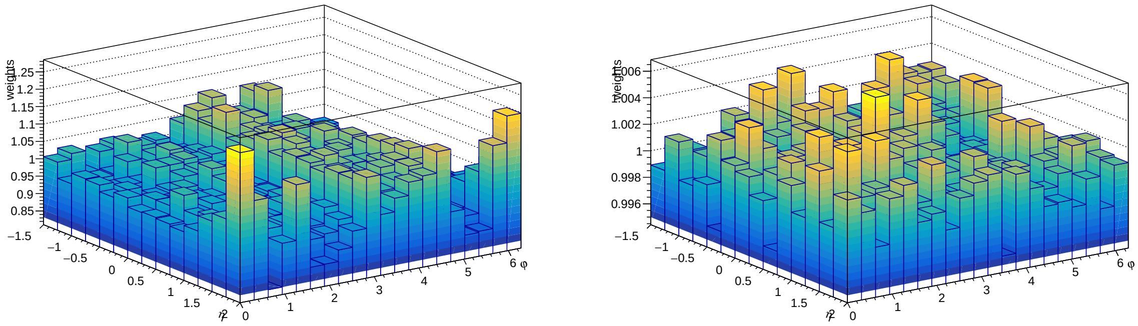

Figure 19: $\eta - \varphi$ *weights. Left: weights as used in analysis. Right: weights as calculated after employing the weights on the left (should be 1). The weights shown here are for positive tracks in DIS events with an event multiplicity of 10.*

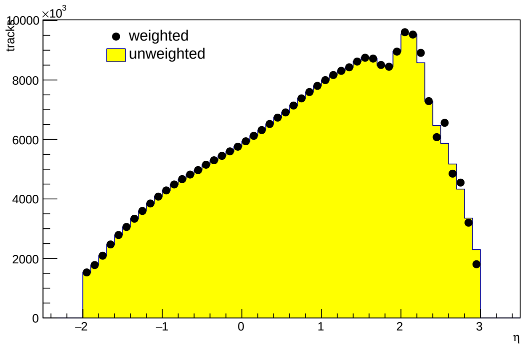

Figure 20: *The* η*-distribution with and without* φ*-weights.*

With the φ-weights, the mean of Q_n-vector should be centered at 0. The $\langle Q_n^{x,y} \rangle$ distributions, corrected and uncorrected, are shown in Figure 21 (for DIS) Figure 69 (for PHP).

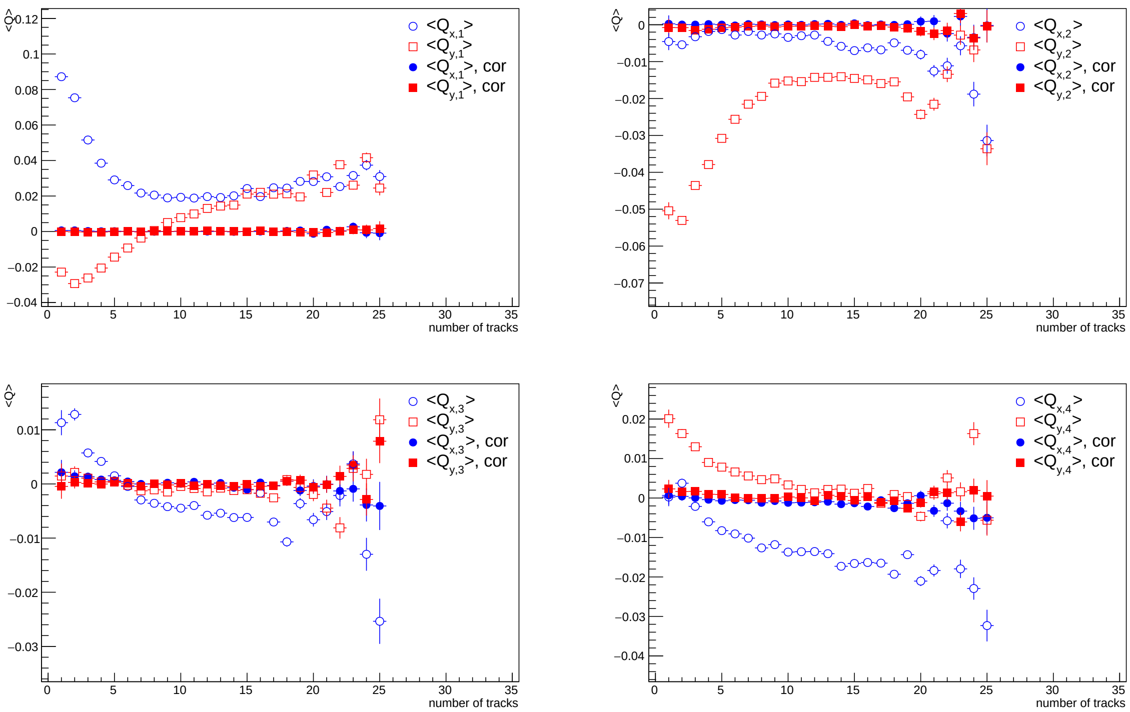

Figure 21: *$\langle Q_{x,y}\rangle$ as a function of event multiplicity for DIS events, showing uncorrected (open symbols) and corrected (full symbols) $\langle Q_{x,y}\rangle$, and clockwise the harmonics $n = 1, 2, 3, 4$.*

The effect of the ϕ-weights on the 2-particle correlation versus multiplicity is shown in Figure 22.

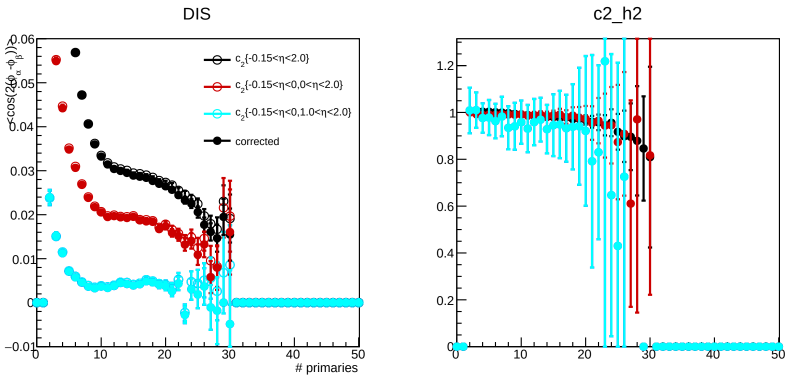

Figure 22: *2-particle correlations with- and without φ-weights.*

The ratio shows that the correction can change the result up to approximately 20% for higher multiplicity events, however the shape of the correlation does not change very much.

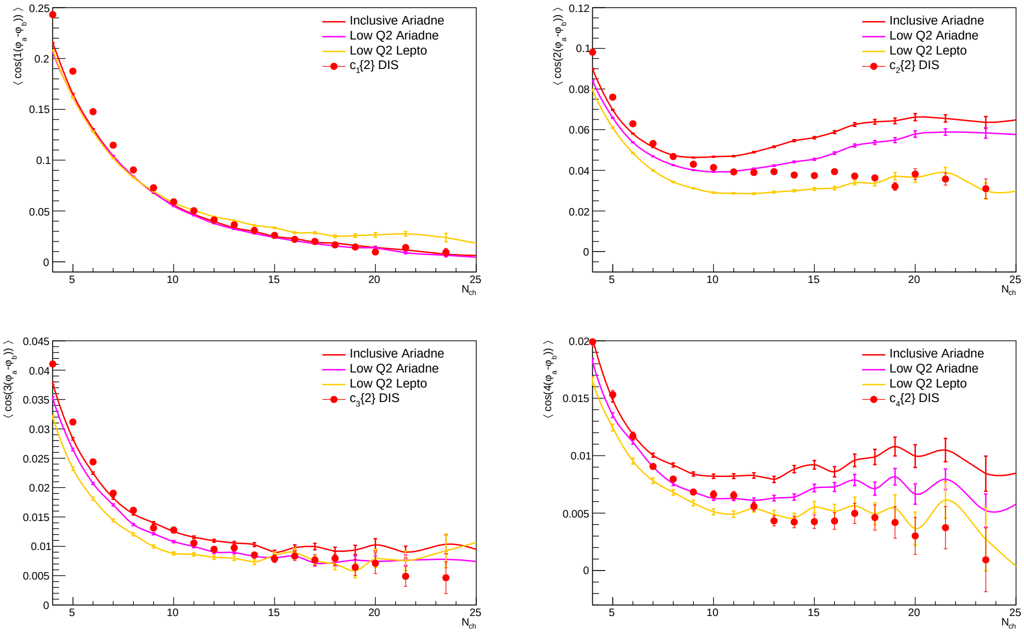

Figure 23: *$c_n\{2\}$ as a function of N_{ch} for $n = 1, 2, 3, 4$.*

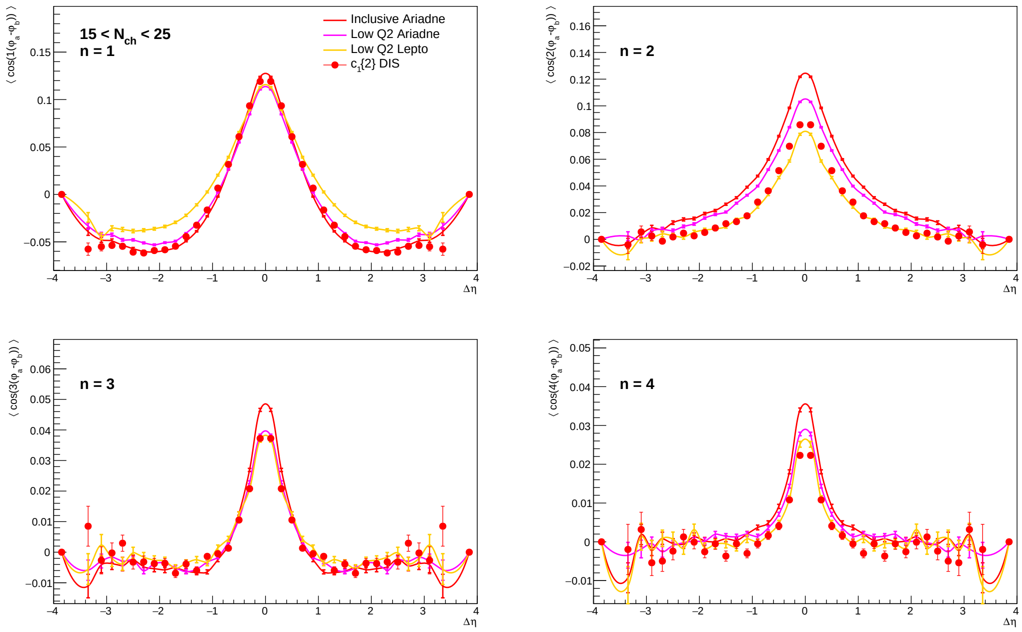

Figure 24: *$c_n\{2\}$ as a function of $\Delta\eta$ for $15 < N_{ch} < 25$ and $n = 1, 2, 3, 4$.*

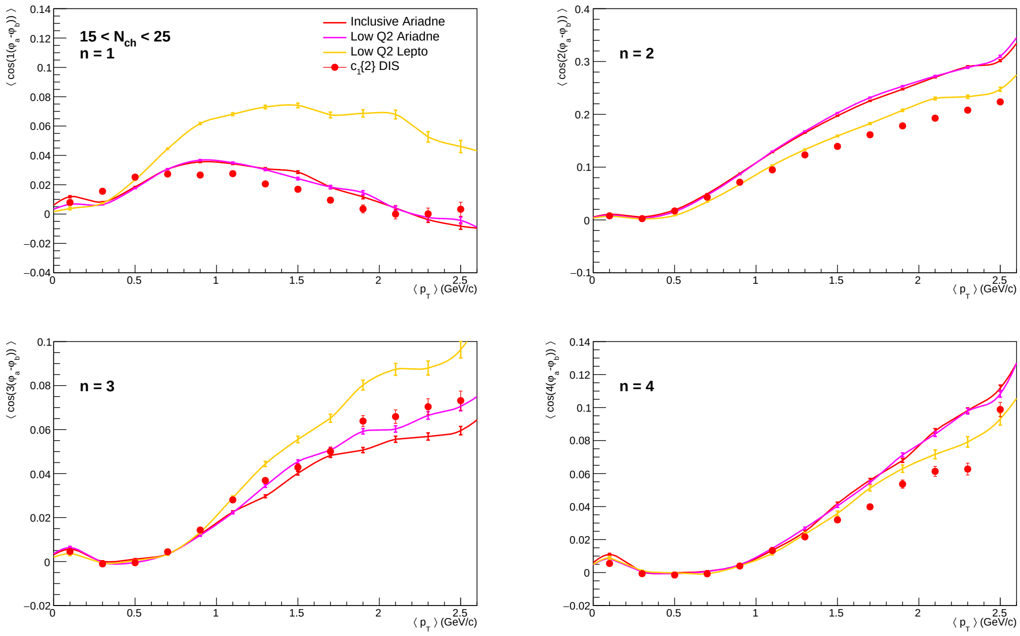

Figure 25: *$c_n\{2\}$ as a function of $\langle p_{\mathrm{T}}\rangle$ for $15 < N_{ch} < 25$ and $n = 1, 2, 3, 4$.*

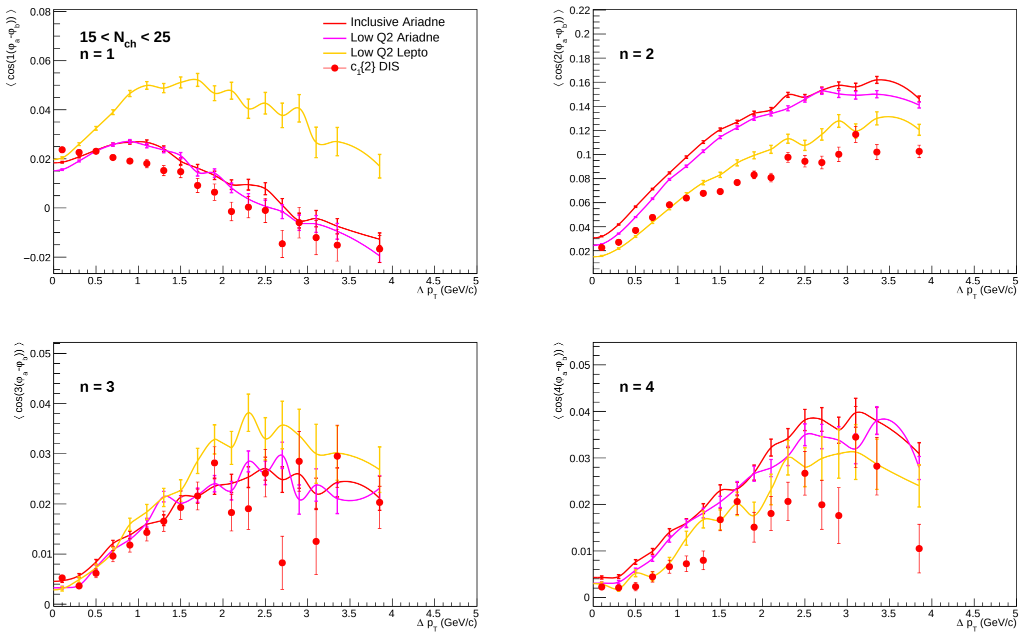

Figure 26: *$c_n\{2\}$ as a function of Δp_{T} for $15 < N_{ch} < 25$ and $n = 1, 2, 3, 4$.*

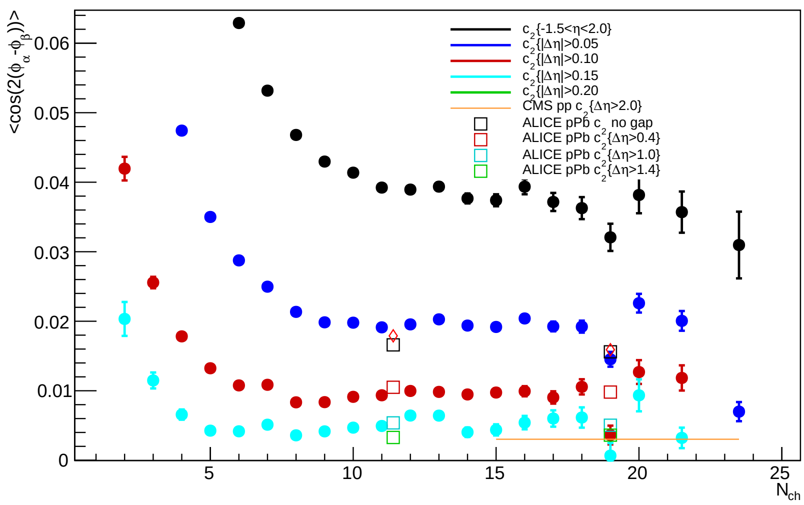

Figure 27: *$c_2\{2\}$ as a function of N_{ch} for different pseudorapidity separation and CMS and ALICE measurements.*

8.1 Complementary two-particle correlations

8.1.1 Integrated vs event multiplicity

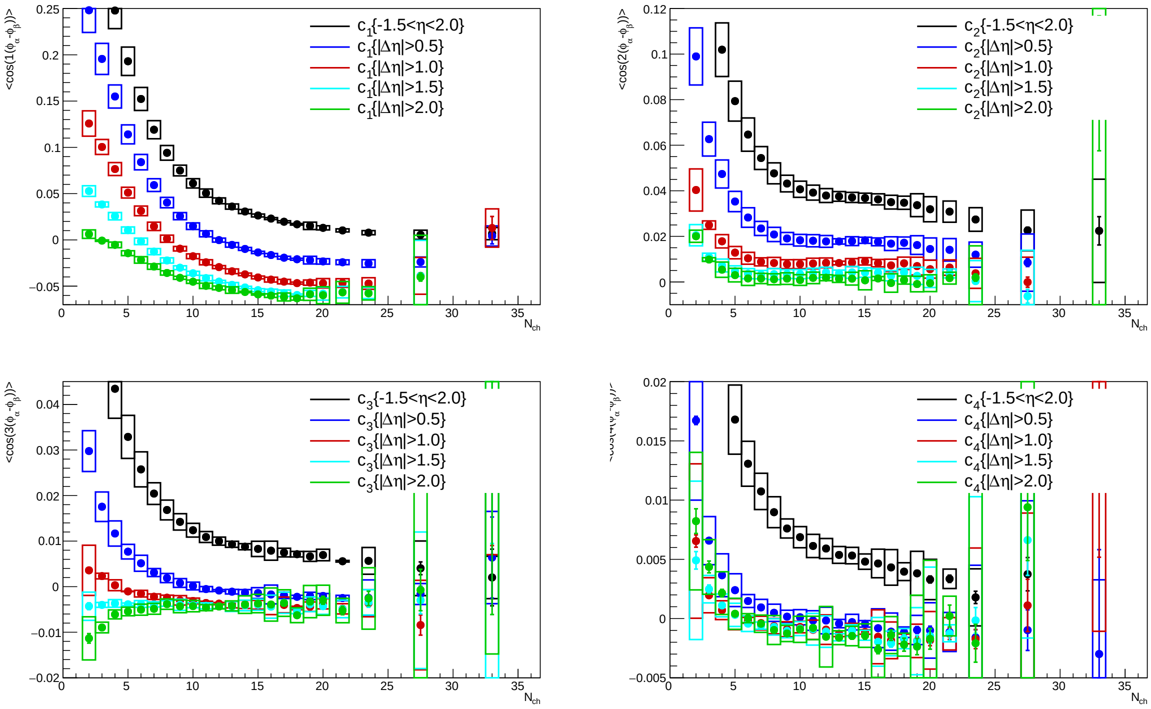

Figure 28: *2-particle correlations versus event multiplicity, with clockwise harmonics* $n = 1, 2, 3, 4$.

8.1.2 Differential in $\Delta\eta$ for various multiplicity ranges

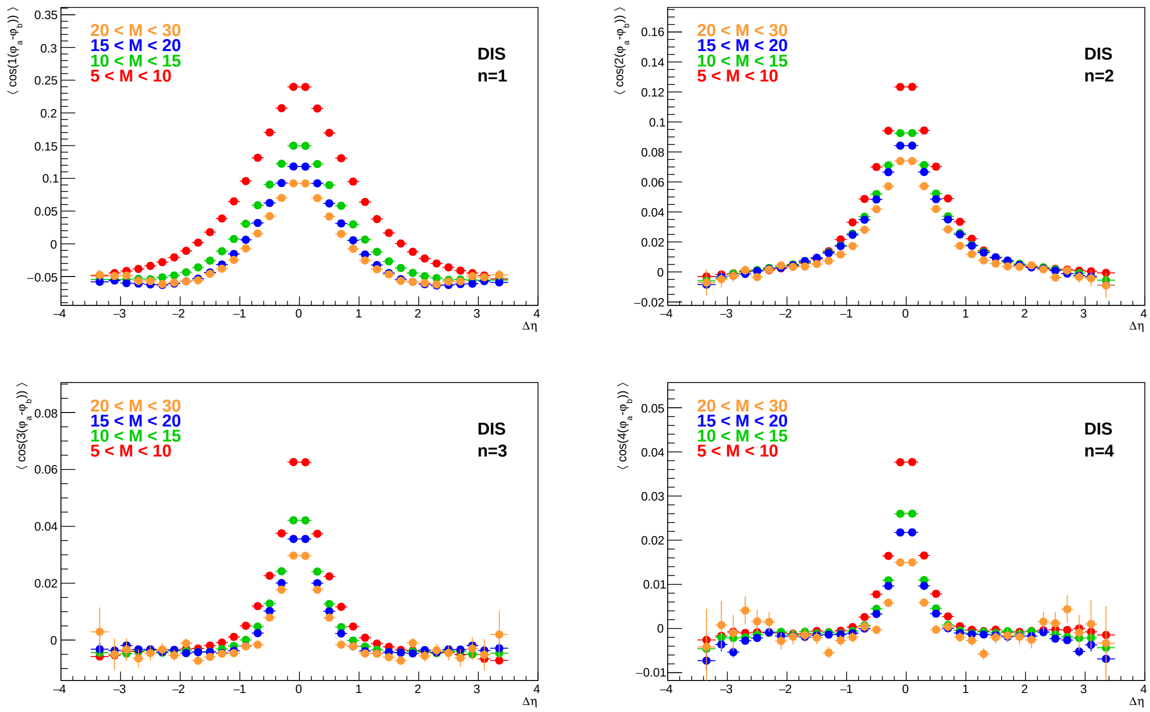

Figure 29: *2-particle correlations versus $\Delta\eta$, left for DIS and right for PHP, with harmonics from top to bottom $n = 1, 2, 3, 4$.*

8.1.3 Differential in Δp_{T} for various multiplicity ranges

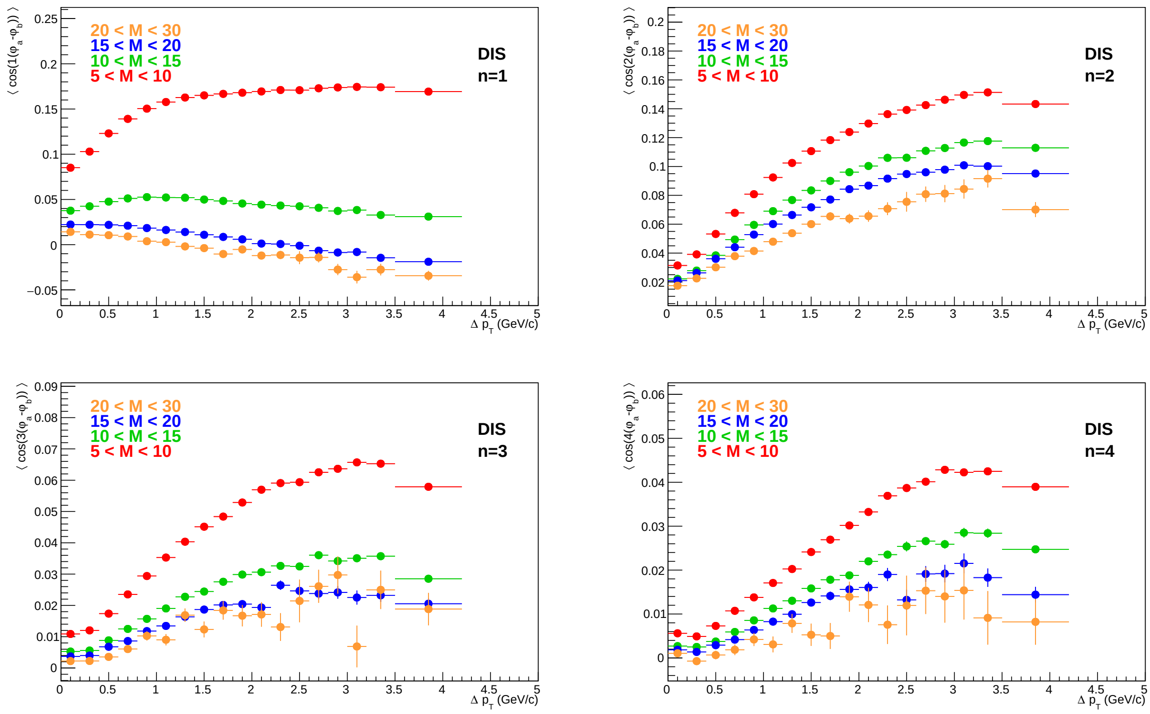

Figure 30: *2-particle correlations versus Δp_{T}, left for DIS and right for PHP, with harmonics from top to bottom $n = 1, 2, 3, 4$.*

8.1.4 Differential in $\langle p_{\mathrm{T}} \rangle$ for various multiplicity ranges

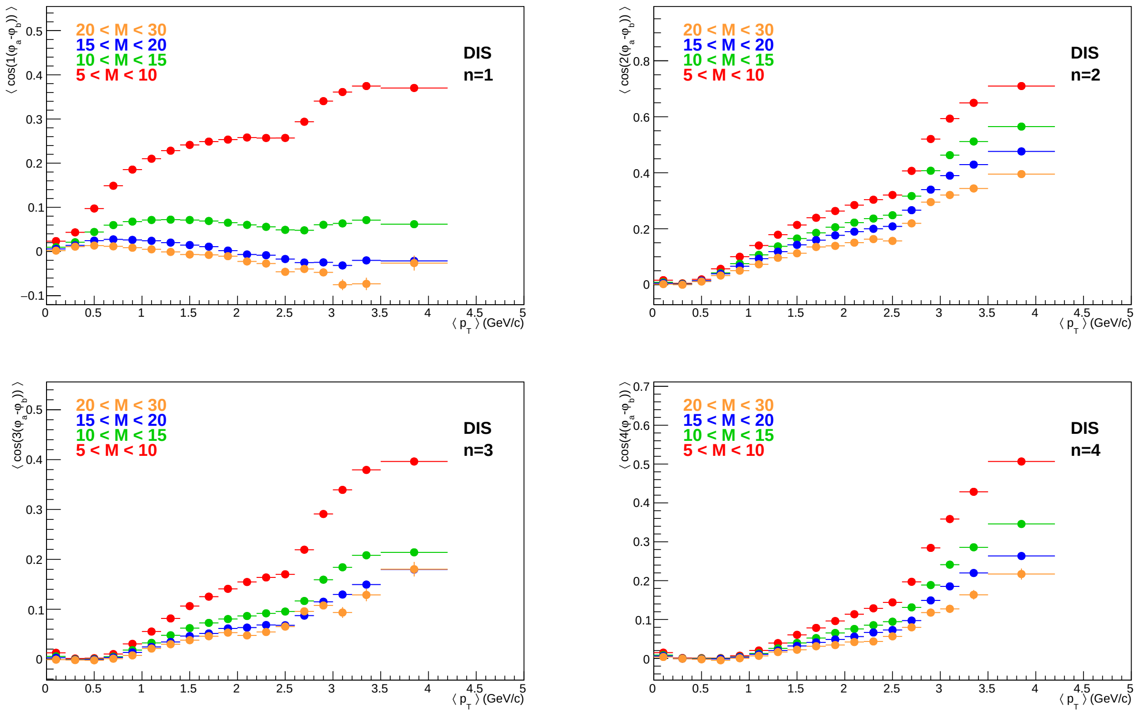

Figure 31: *2-particle correlations versus $\langle p_{\mathrm{T}} \rangle$, left for DIS and right for PHP, with harmonics from top to bottom $n = 1, 2, 3, 4$.*

8.2 Model comparison

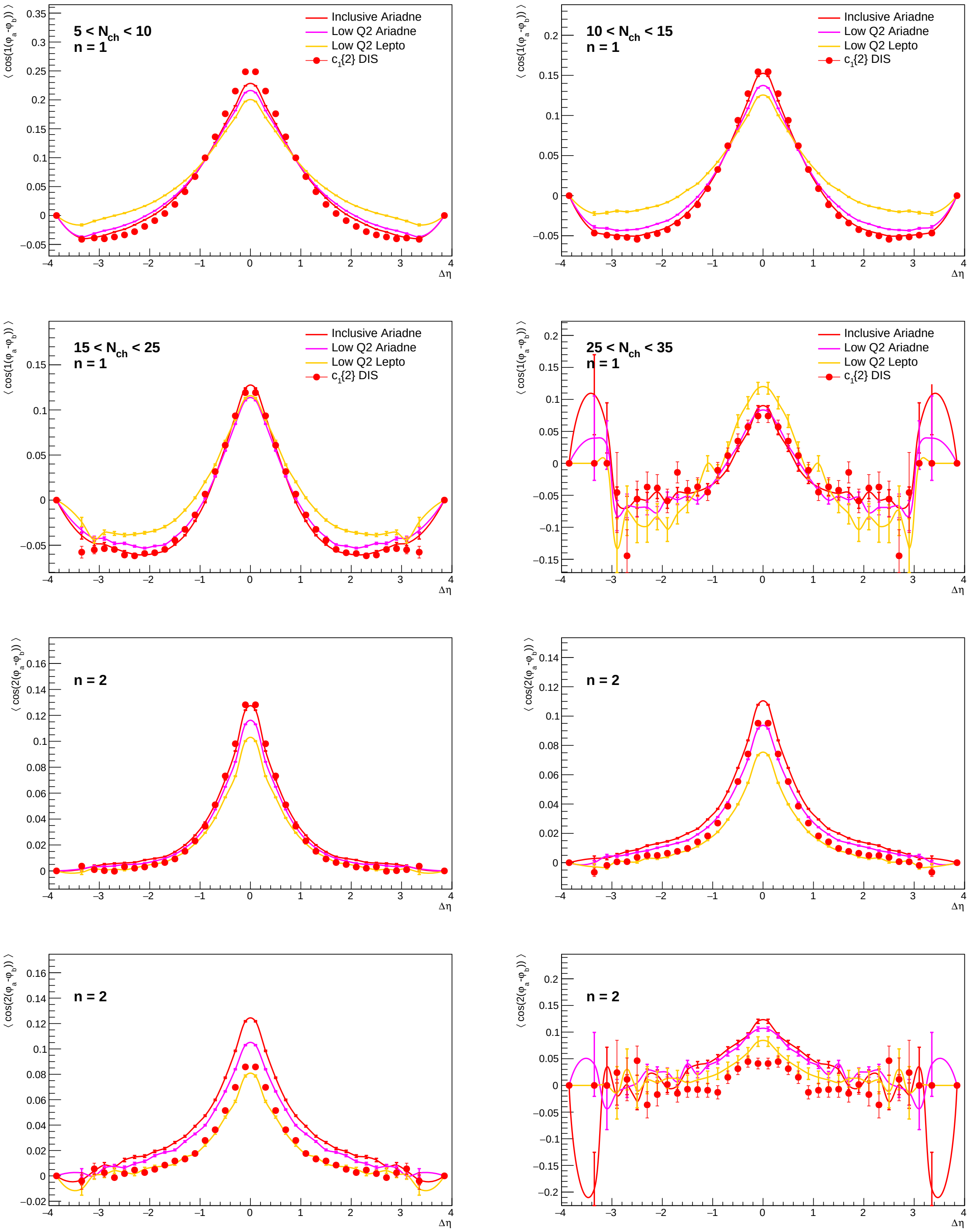

Figure 32: *Differential in* $\Delta\eta$ *for harmonics* $n = 1, 2$, *with varying multiplicity ranges from top to bottom.*

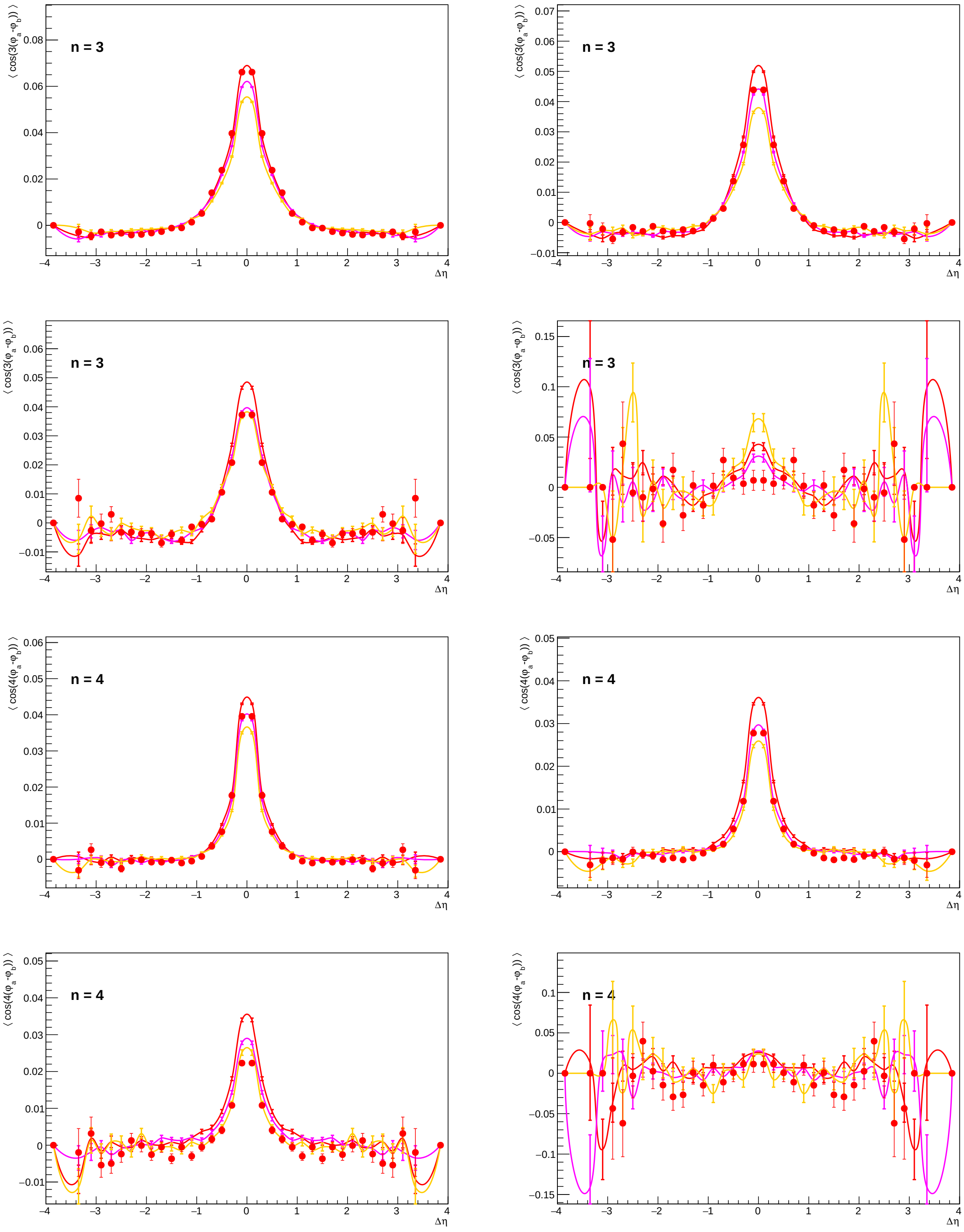

Figure 33: *Differential in* $\Delta\eta$ *for harmonics* $n = 3, 4$, *with varying multiplicity ranges from top to bottom.*

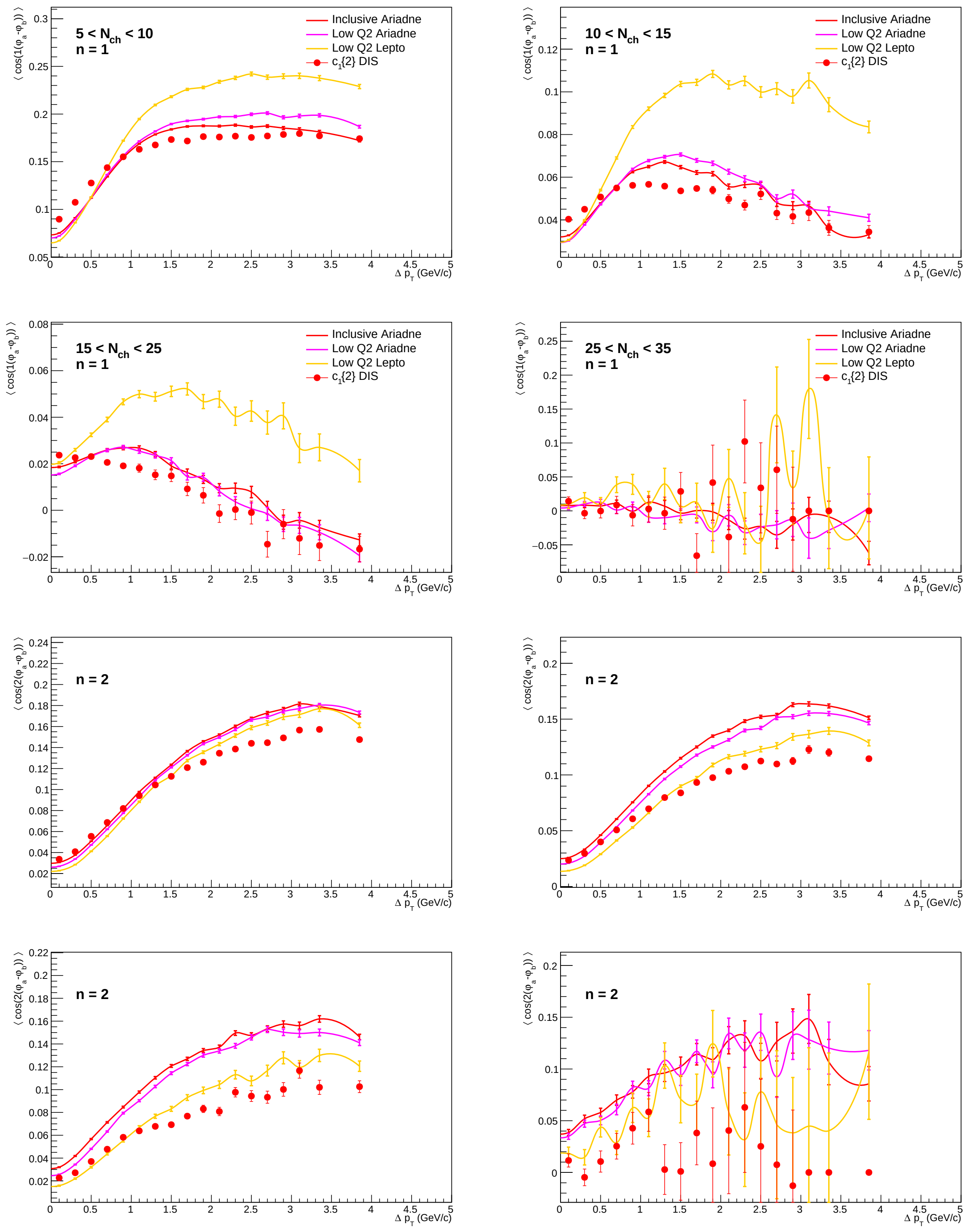

Figure 34: *Differential in* Δp_{T} *for harmonics* $n = 1, 2$, *with varying multiplicity ranges from top to bottom.*

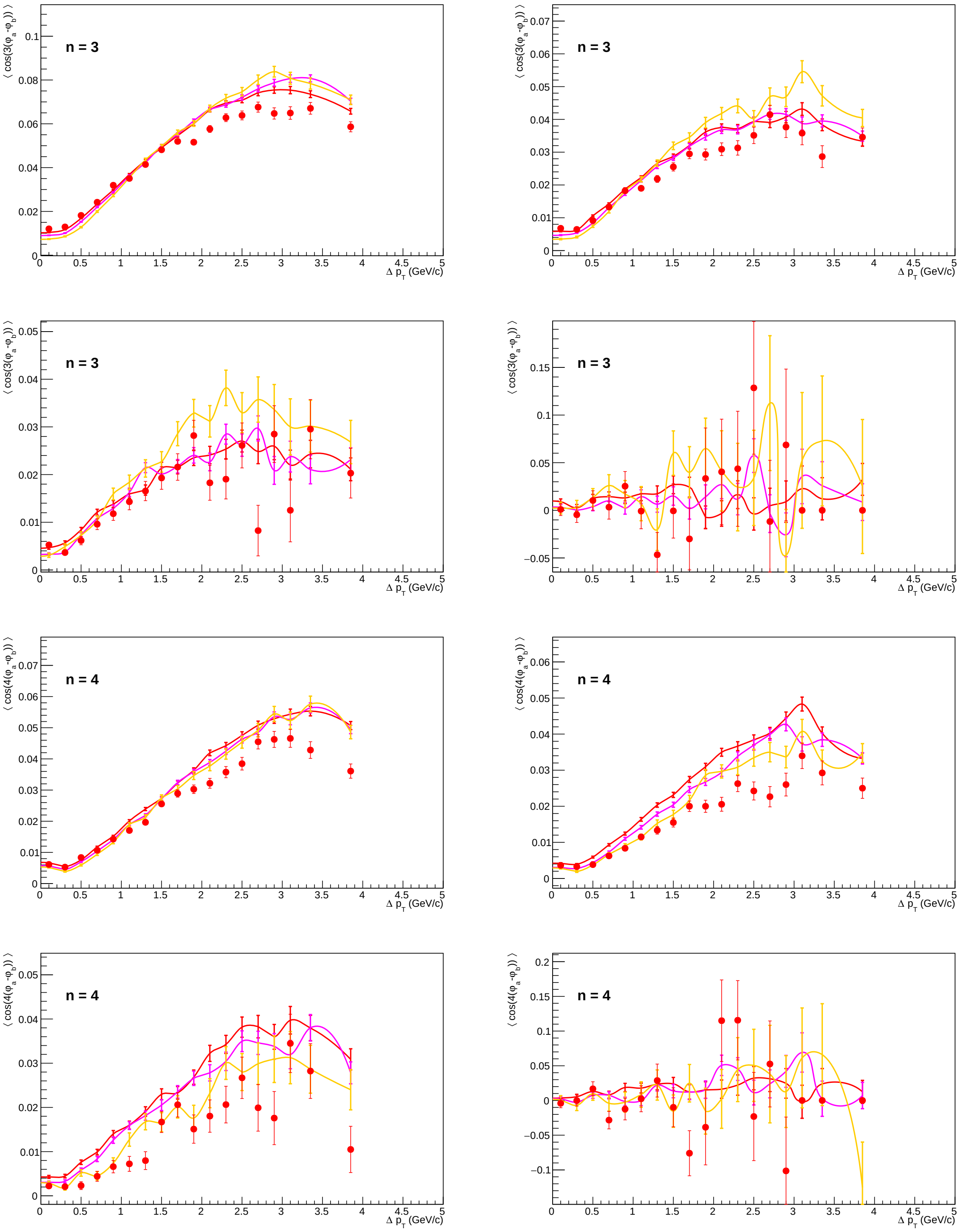

Figure 35: *Differential in* Δp_{T} *for harmonics* $n = 3, 4$, *with varying multiplicity ranges from top to bottom.*

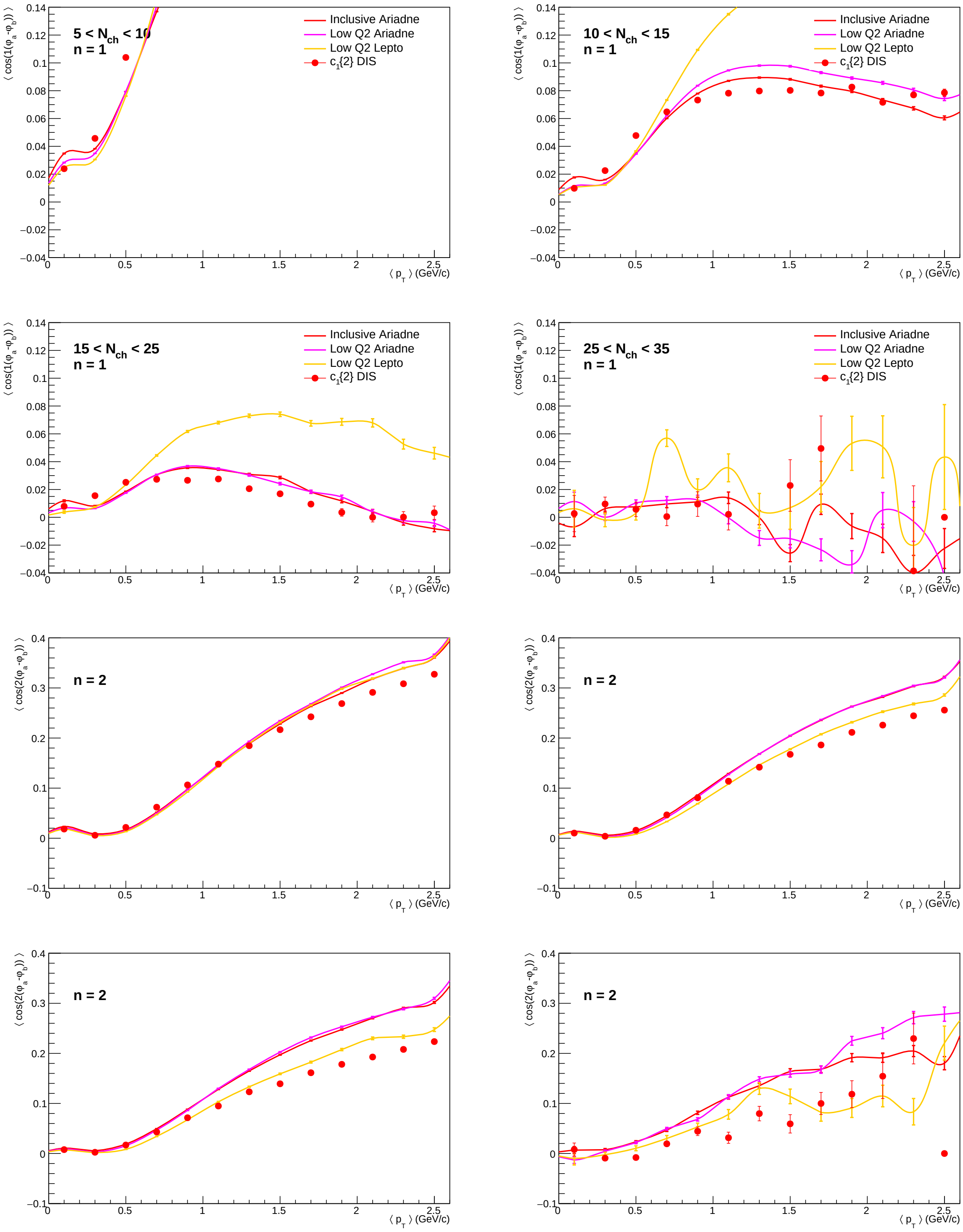

Figure 36: *Differential in $\langle p_{\mathrm{T}} \rangle$ for harmonics $n = 1, 2$, with varying multiplicity ranges from top to bottom.*

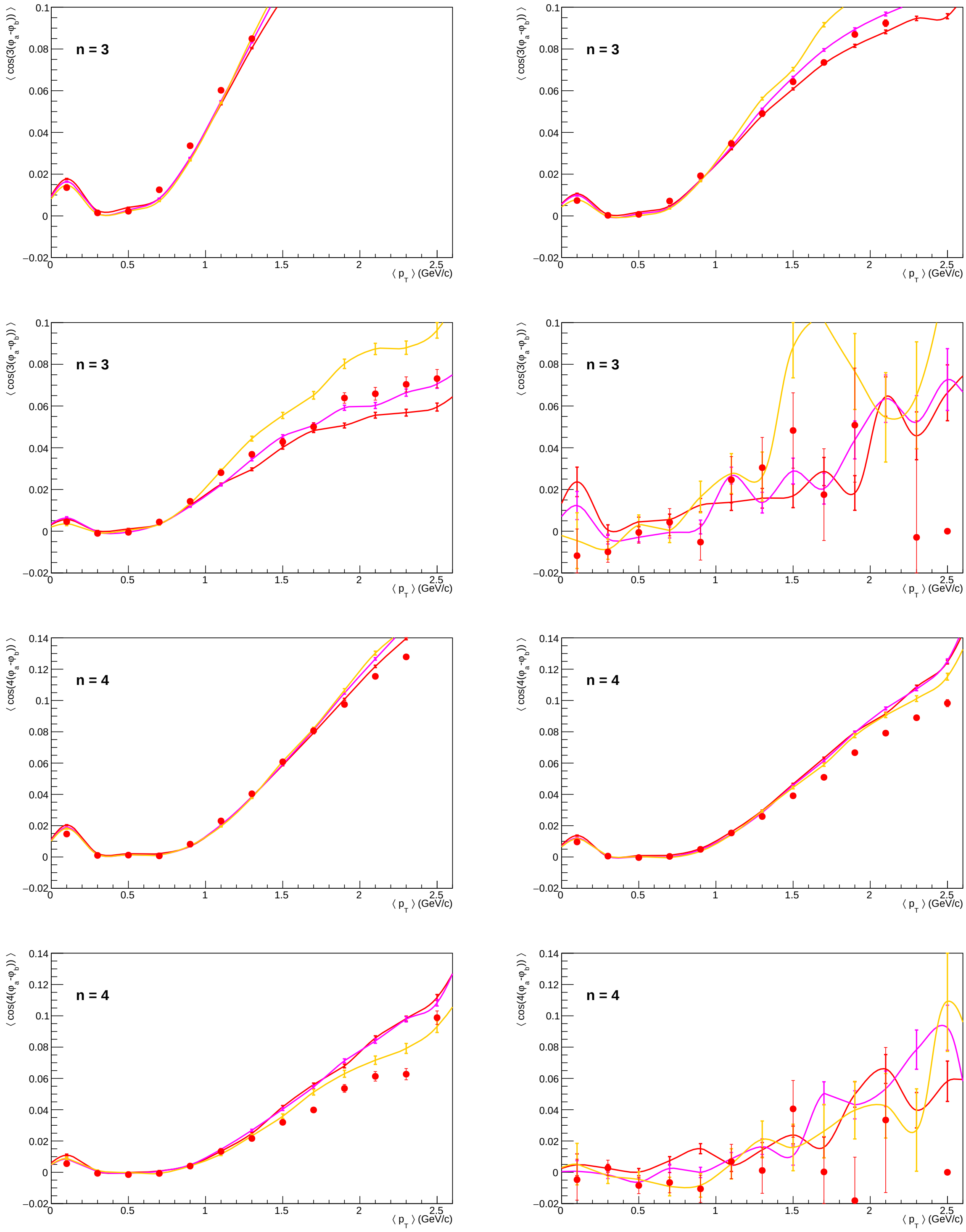

Figure 37: *Differential in* $\langle p_{\mathrm{T}} \rangle$ *for harmonics* $n = 3, 4$*, with varying multiplicity ranges from top to bottom.*

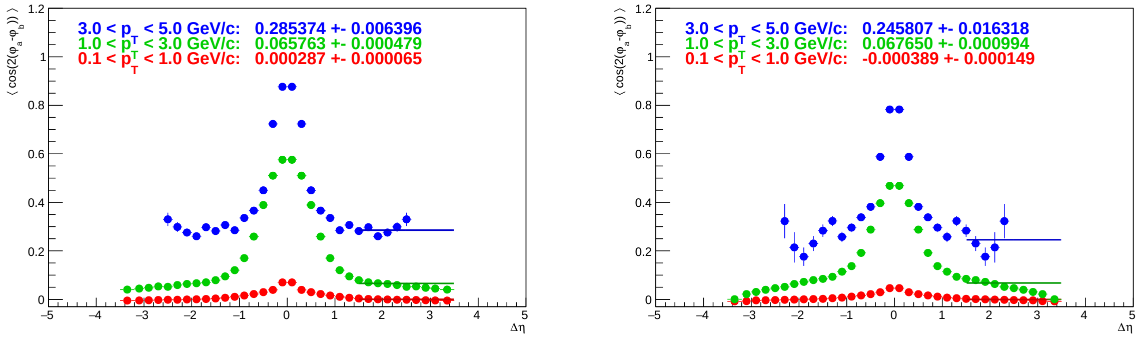

Figure 38: *2-particle correlations versus $\Delta\eta$, in 3 p_{T} ranges (see legend) and in 2 multiplicity ranges (left $5 < M < 15$, right $15 < M < 30$. The fit results are for pol0 fits in the η-range of 1.5 to 3.5*

325 The shape of the correlation for the higher multiplicity event (right side) is clearly teeper towards higher $\Delta\eta$, especially for $1.0 < p_{\mathrm{T}} < 3.0$ GeV/c.

9 Systematics

To study the systematic uncertainty in the measurement, we vary event and track selection and add deviations in quadrature for a conservative estimate (for the moment).

9.1 Trigger bias

To understand how the trigger selection affects the measurement, we have a look at the physics observables before, and after trigger selection. All generated tracks from all MC events (ari_incl_nc_DIS_lowQ2) are considered, and compared to generated tracks from events that pass the DIS trigger selection.

In the following Figure 55, we check the measurement of the 2-particle correlation for various η-gaps, using generated particles and reconstructed particles, for different harmonics.

Clearly there are significant differences between the measurements for generated and reconstructed particles. Corrections for tracking efficiency have not yet been applied in this comparison. But it seems obvious that large differences will remain. Whether it is correlations from secondaries or a trigger bias is to be investigated.

We look at the bias from trigger/event selection by comparing the correlation between generated particles before and after the selection:

We look at the bias purely from reconstruction by comparing the correlation between generated particles and reconstructed particles after the selection:

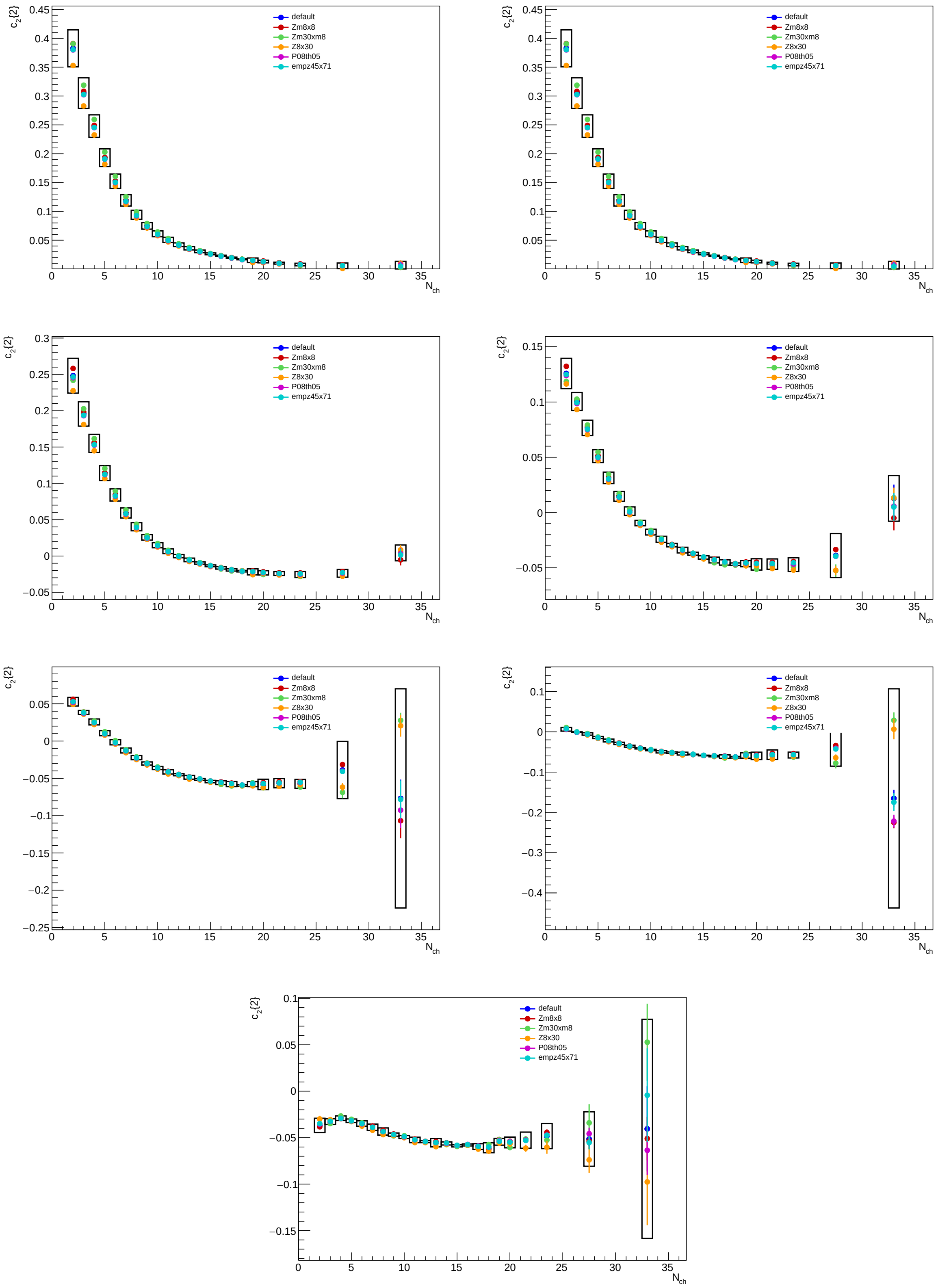

Figure 39: *Contributions to the systematic uncertainty for* $n = 1$ *for different* $\eta-$*separation.*

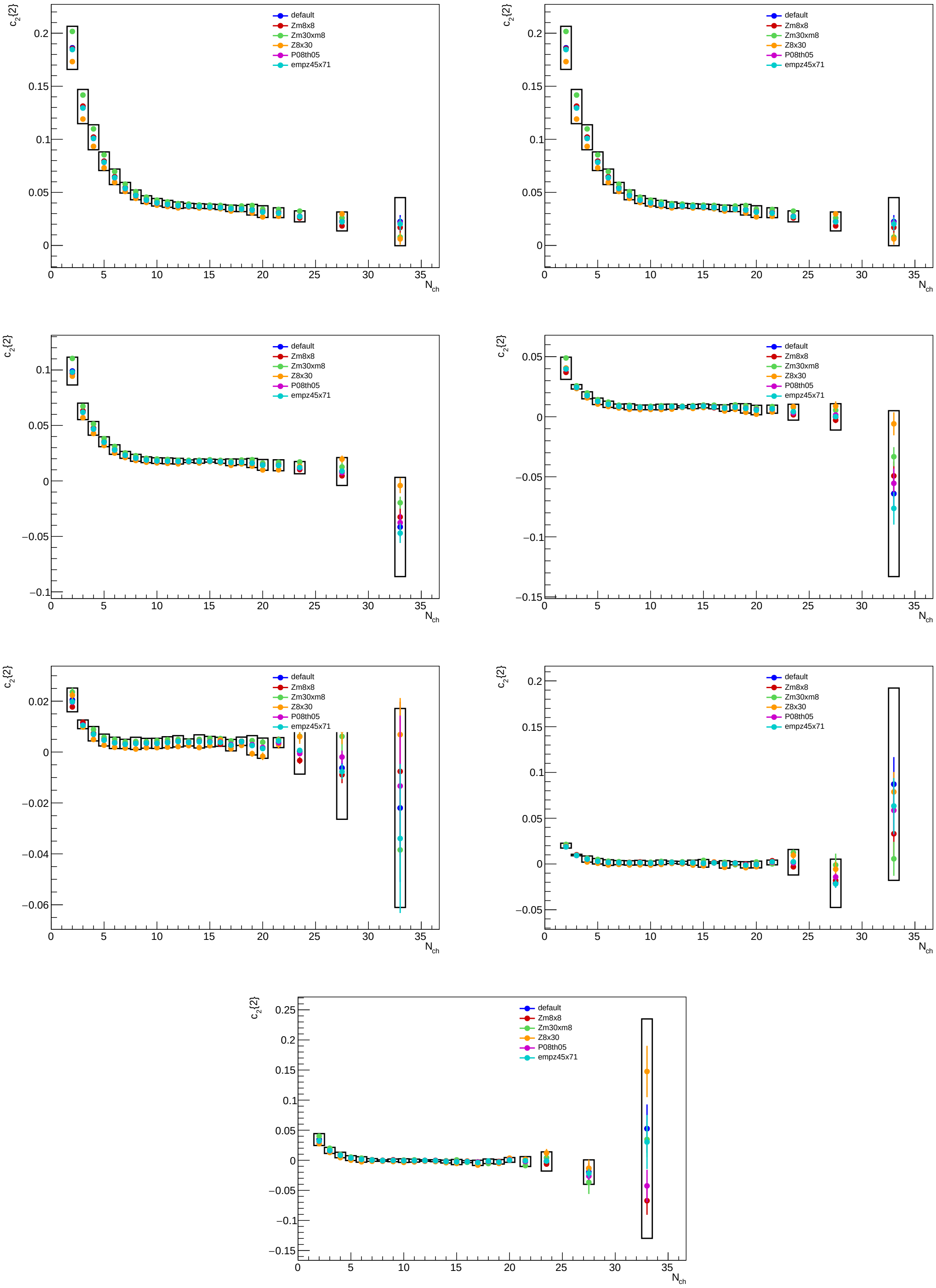

Figure 40: *Contributions to the systematic uncertainty for $n = 2$ for different $\eta-$separation.*

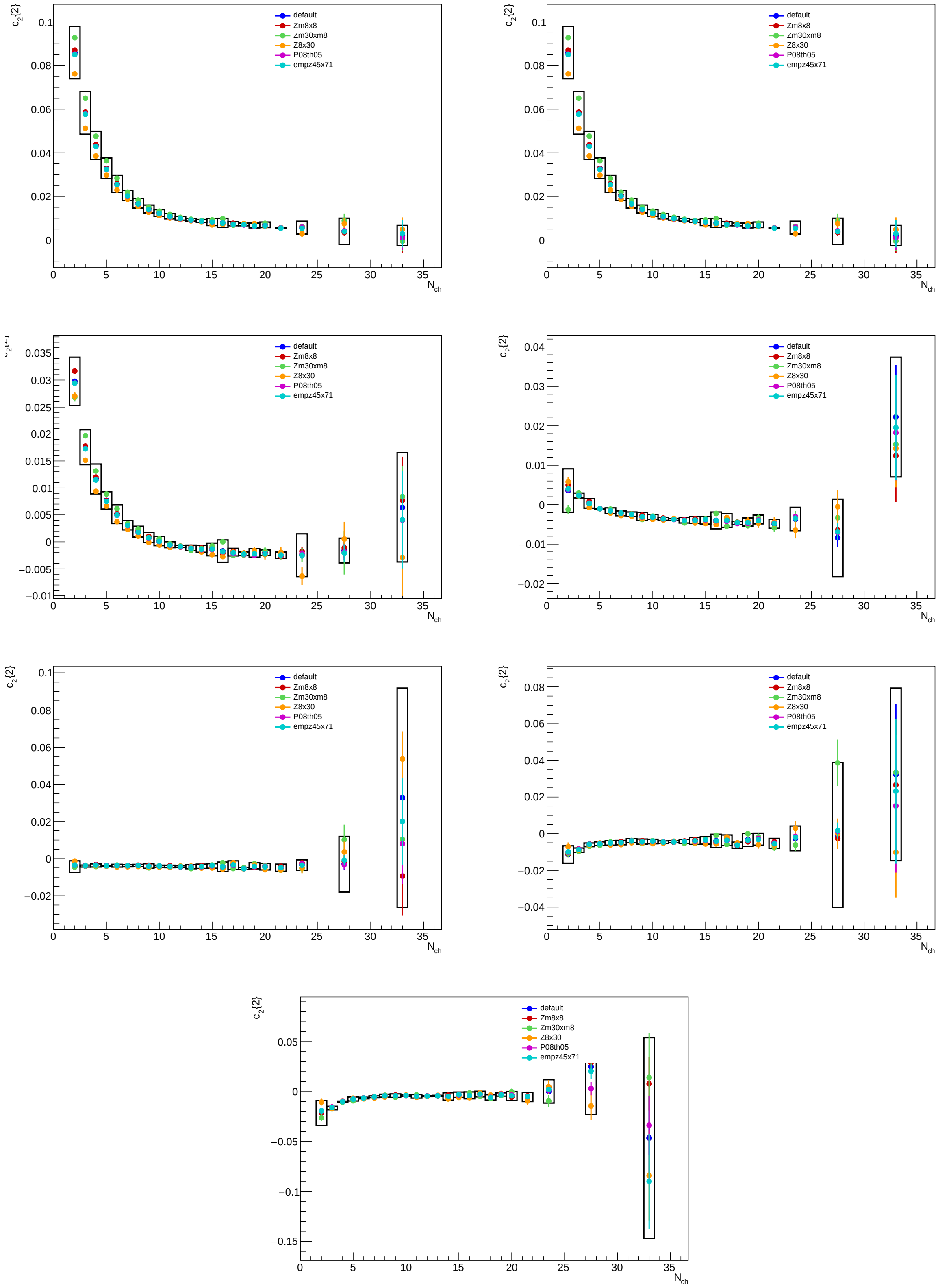

Figure 41: *Contributions to the systematic uncertainty for* $n = 3$ *for different* $\eta-$*separation.*

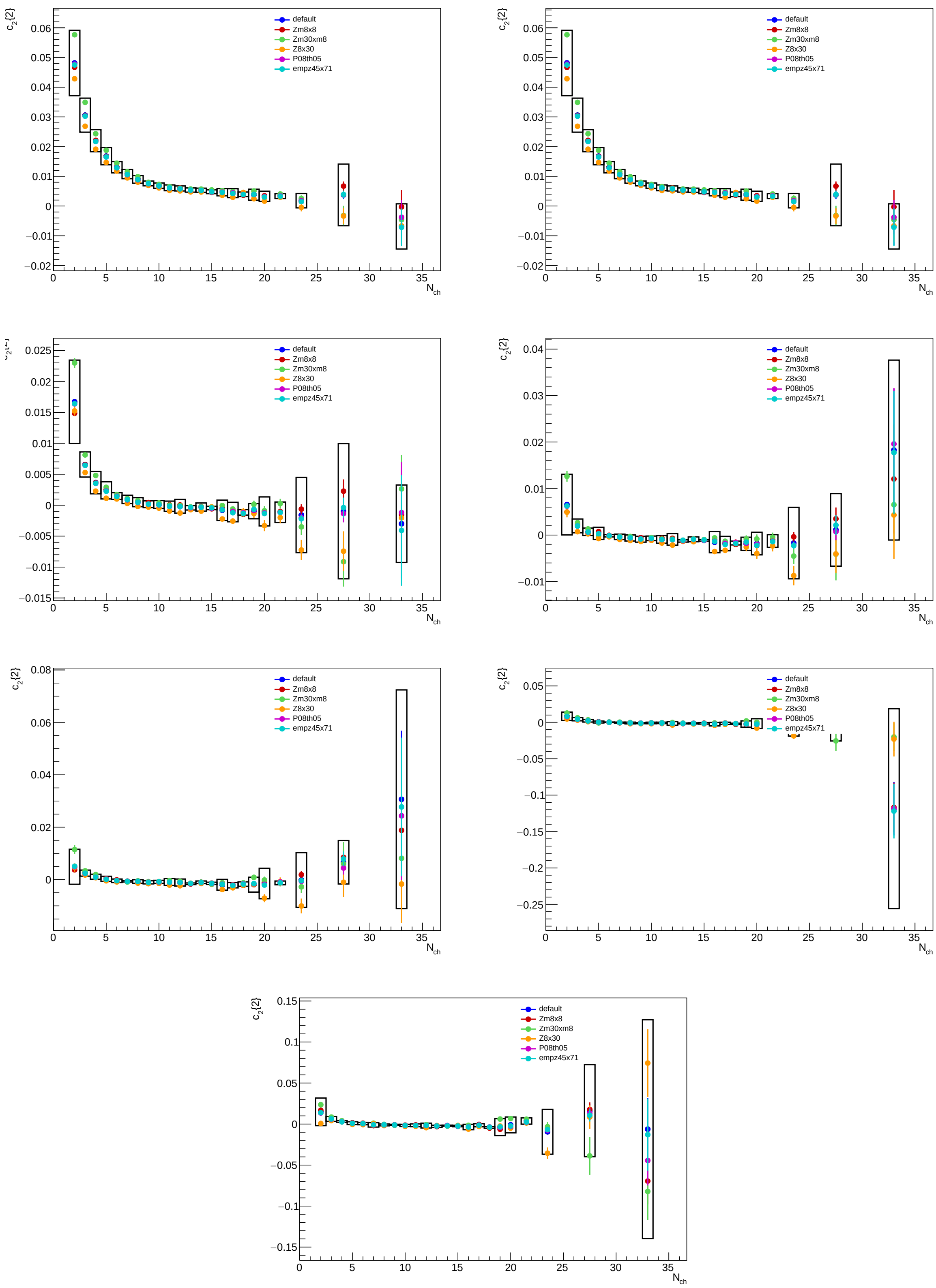

Figure 42: *Contributions to the systematic uncertainty for* $n = 4$ *for different* $\eta-$*separation.*

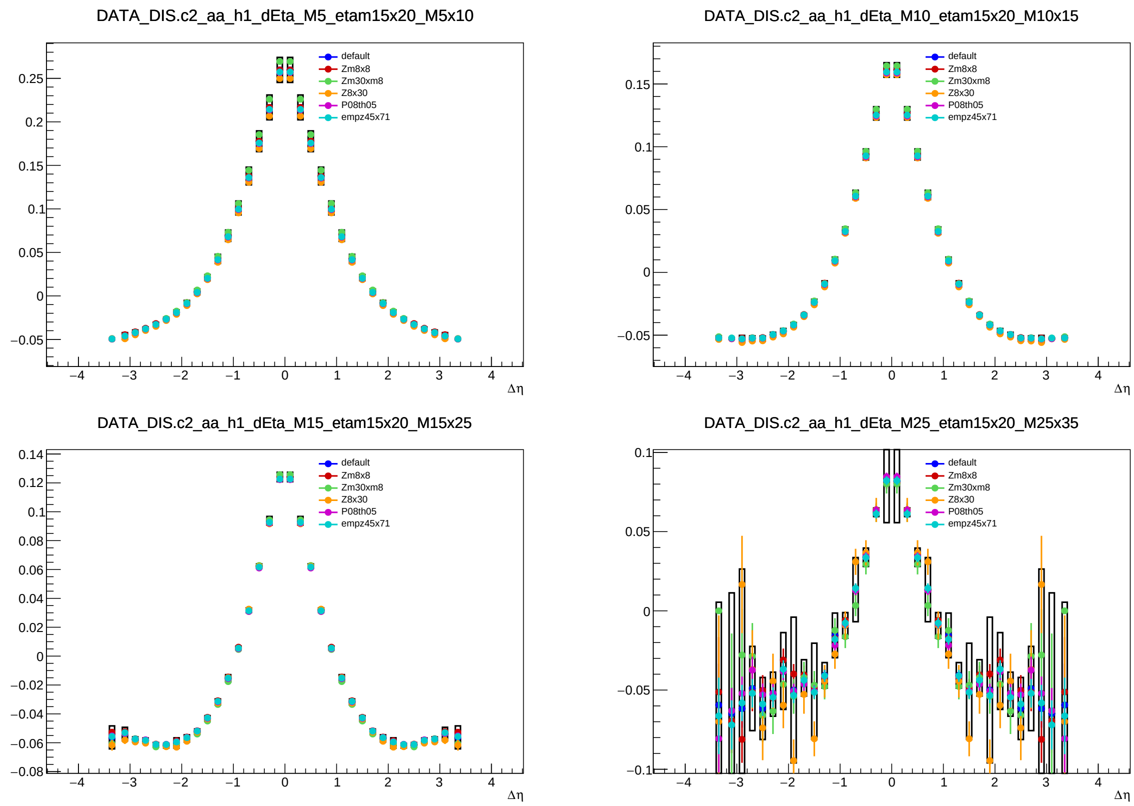

Figure 43: *Contributions to the systematic uncertainty for* $n = 1$ *for different multiplicities.*

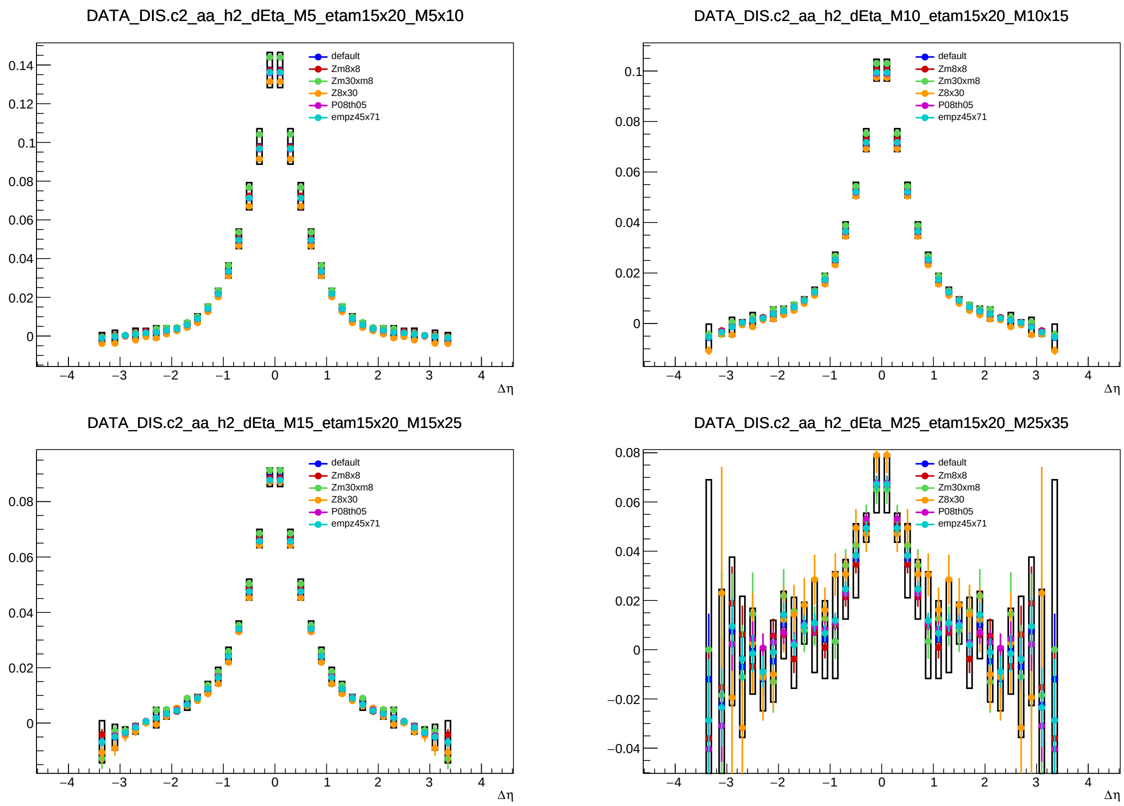

Figure 44: *Contributions to the systematic uncertainty for* $n = 2$ *for different multiplicities.*

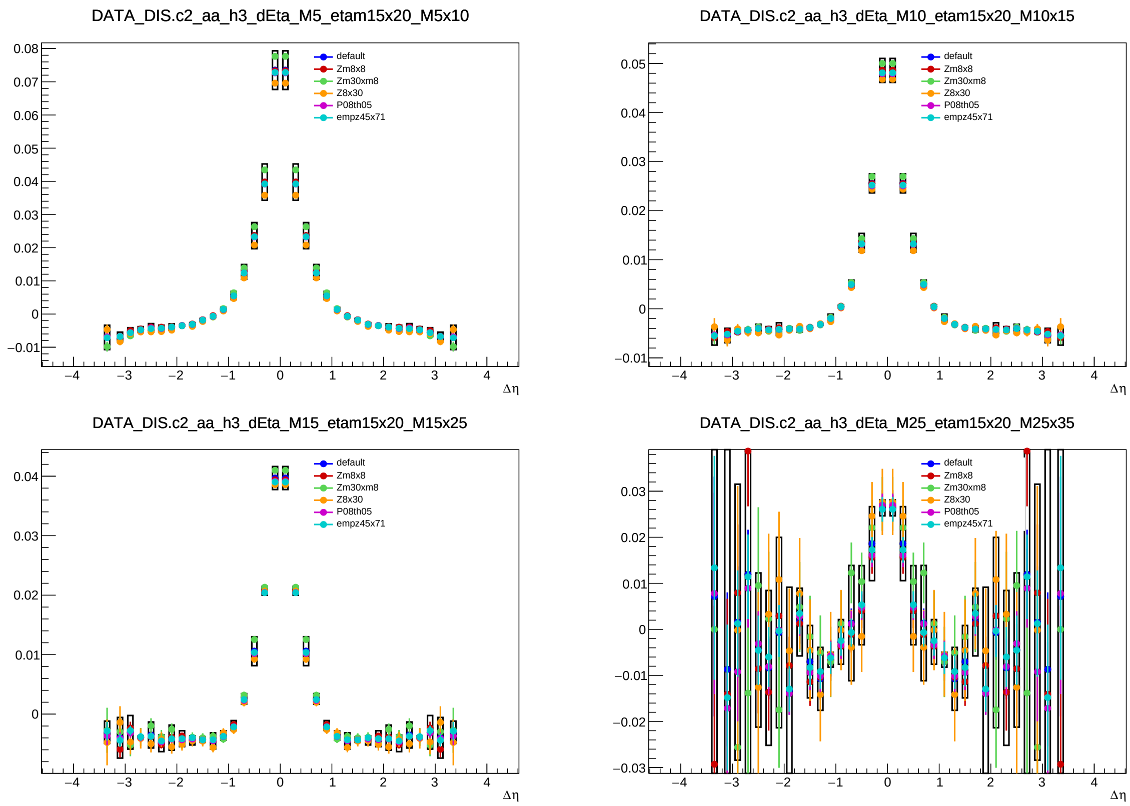

Figure 45: *Contributions to the systematic uncertainty for* $n = 3$ *for different multiplicities.*

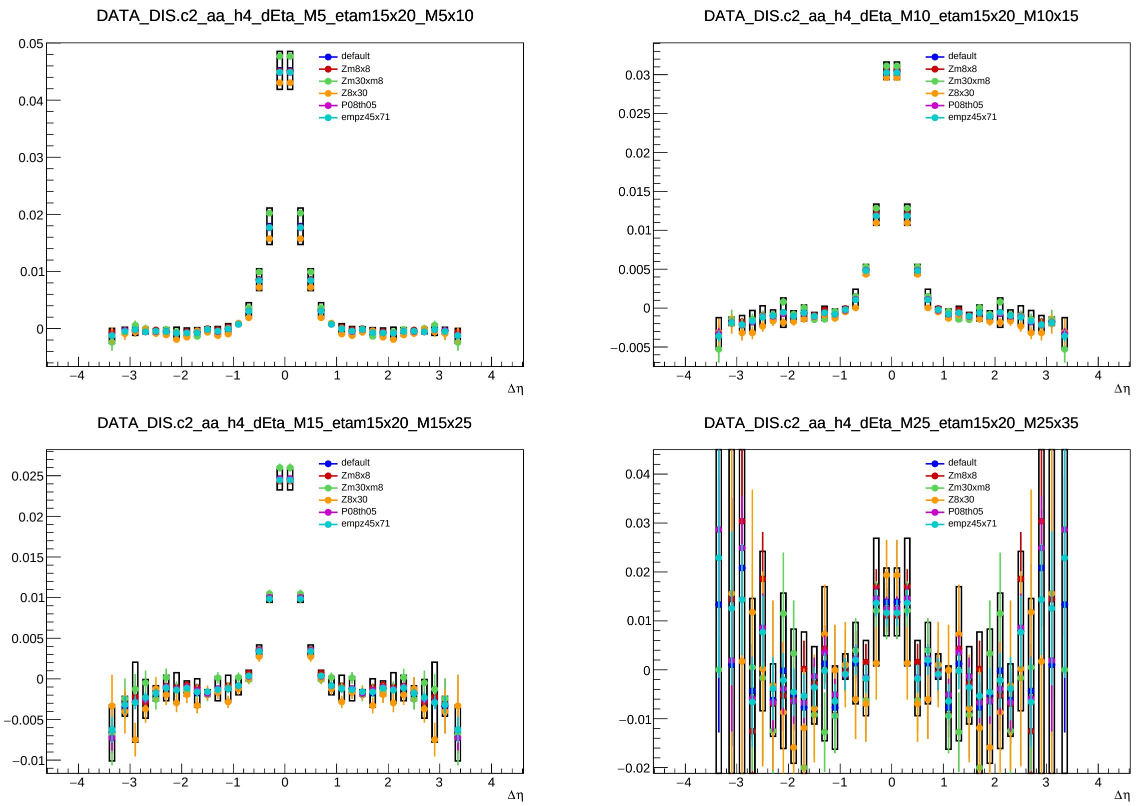

Figure 46: *Contributions to the systematic uncertainty for $n = 4$ for different multiplicities.*

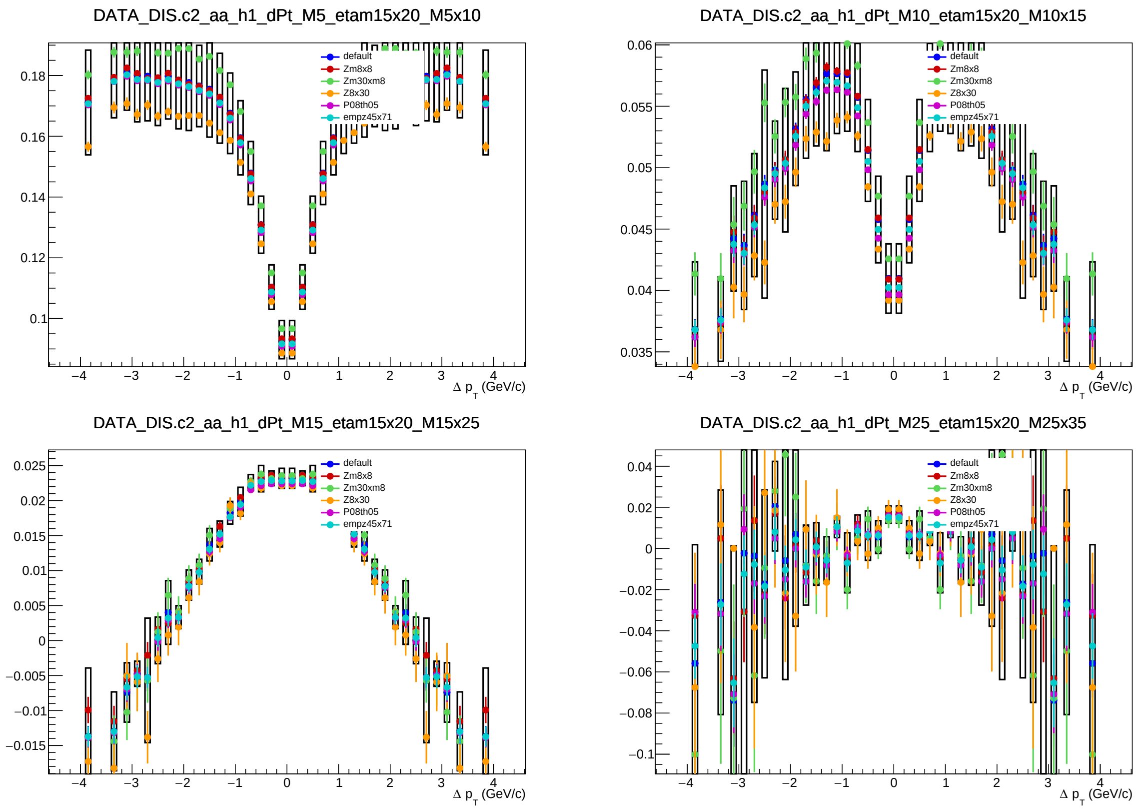

Figure 47: *Contributions to the systematic uncertainty for* $n = 1$ *for different multiplicities.*

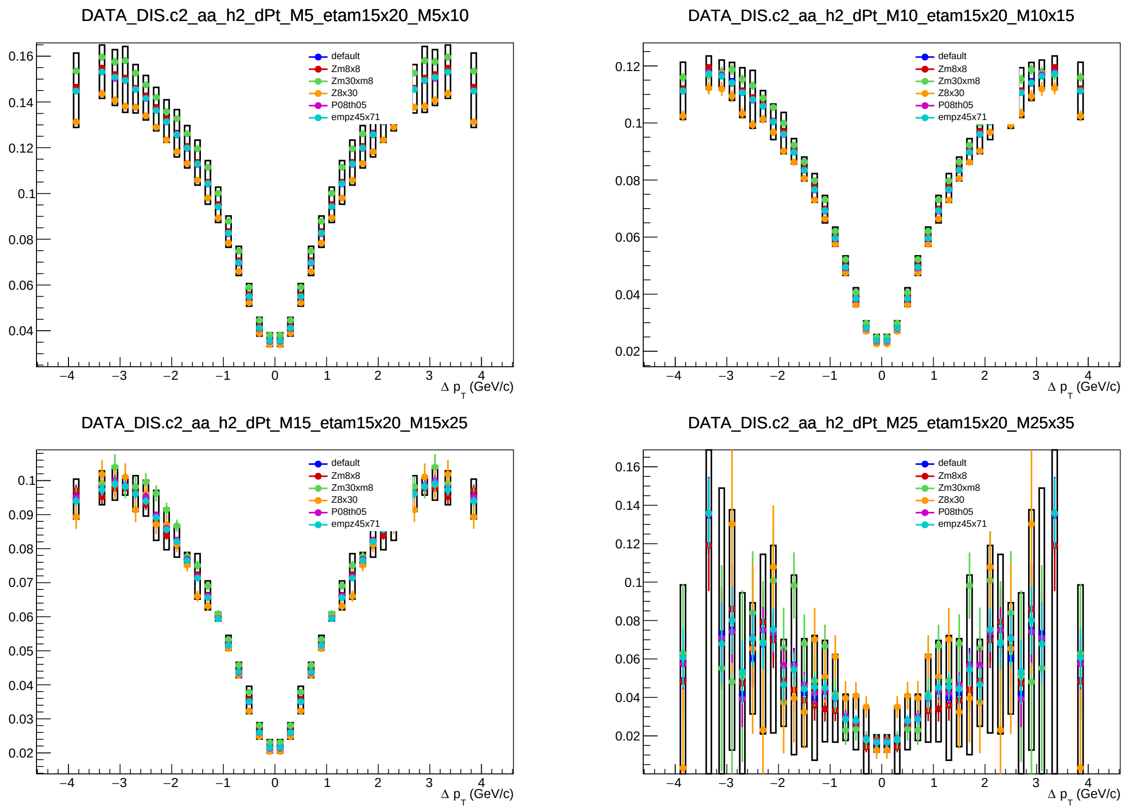

Figure 48: *Contributions to the systematic uncertainty for* $n = 2$ *for different multiplicities.*

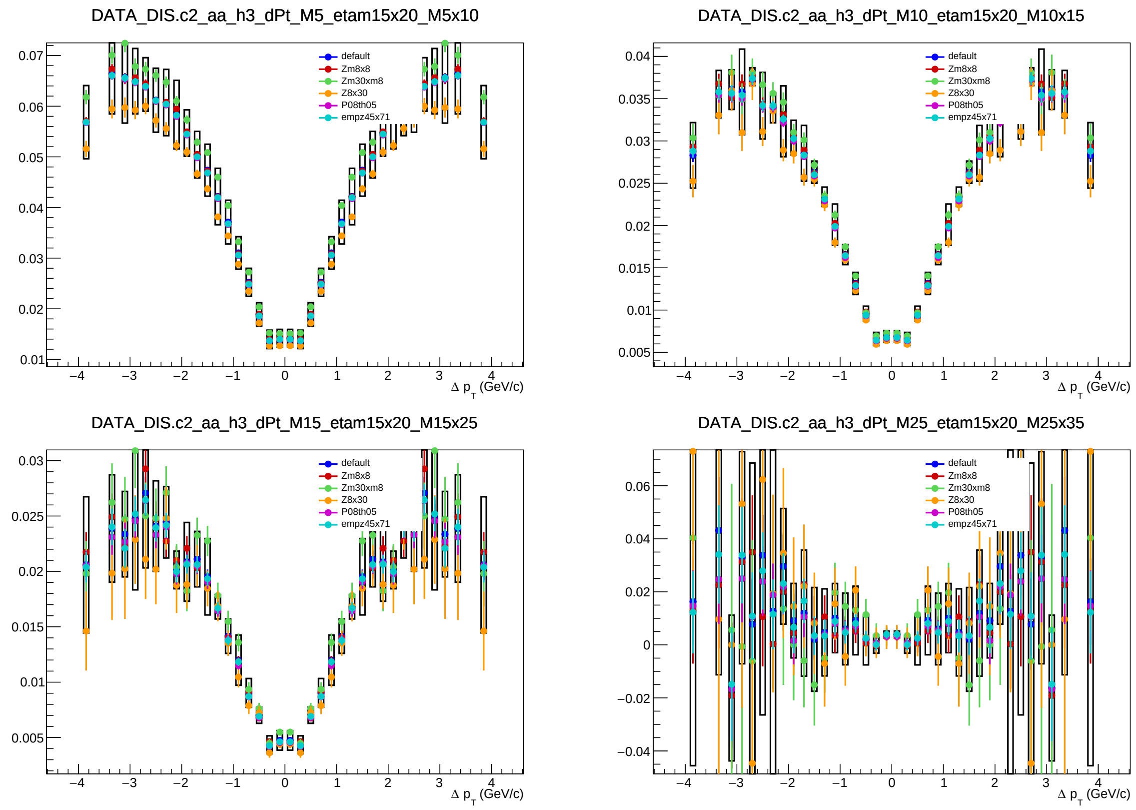

Figure 49: *Contributions to the systematic uncertainty for* $n = 3$ *for different multiplicities.*

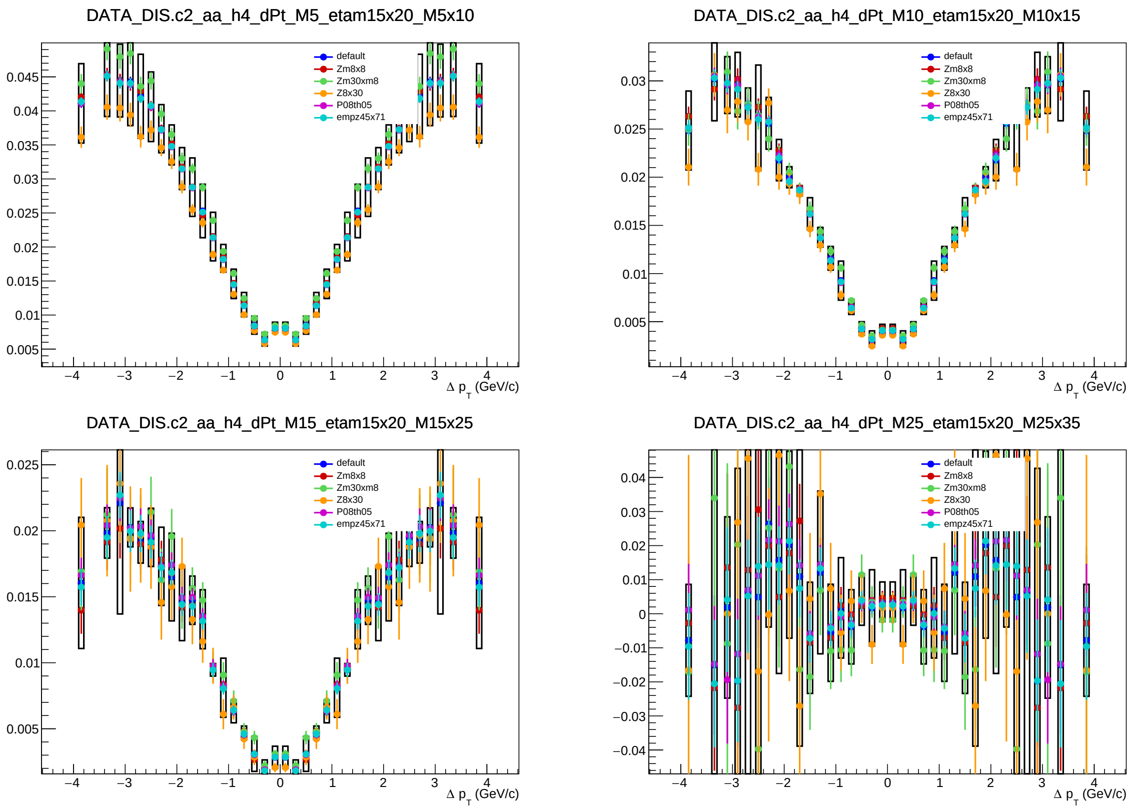

Figure 50: *Contributions to the systematic uncertainty for* $n = 4$ *for different multiplicities.*

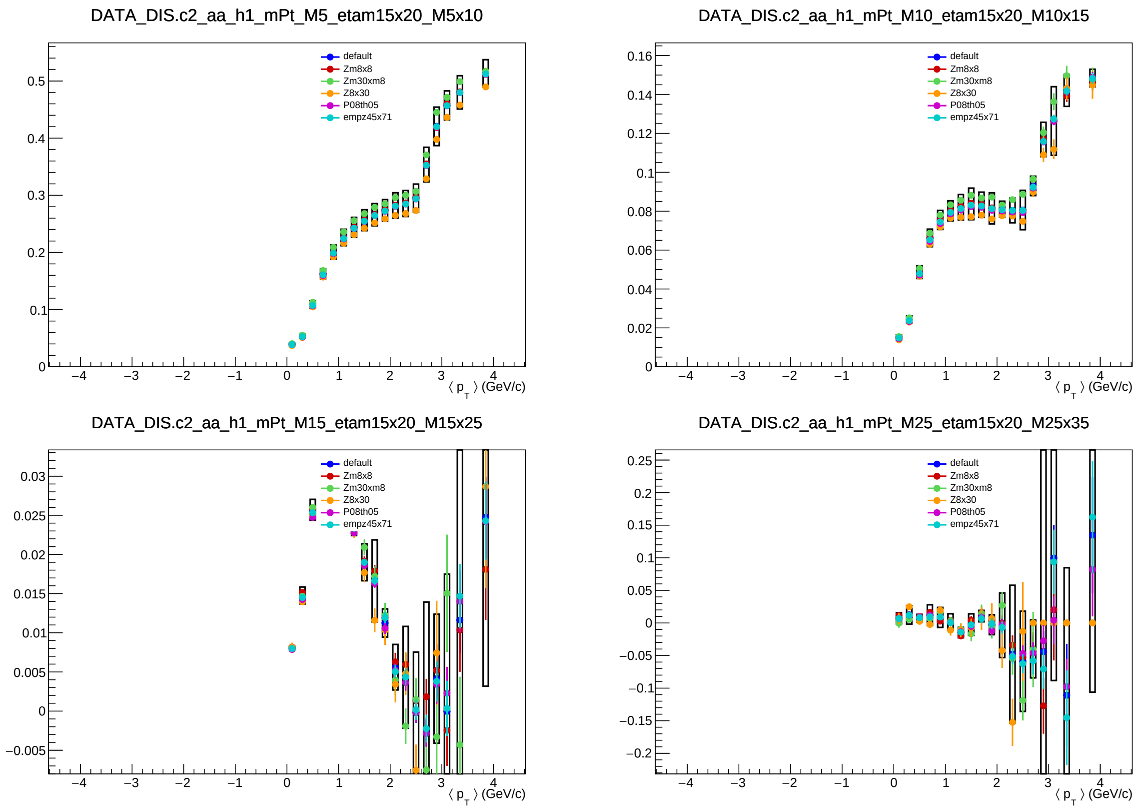

Figure 51: *Contributions to the systematic uncertainty for $n = 1$ for different multiplicities.*

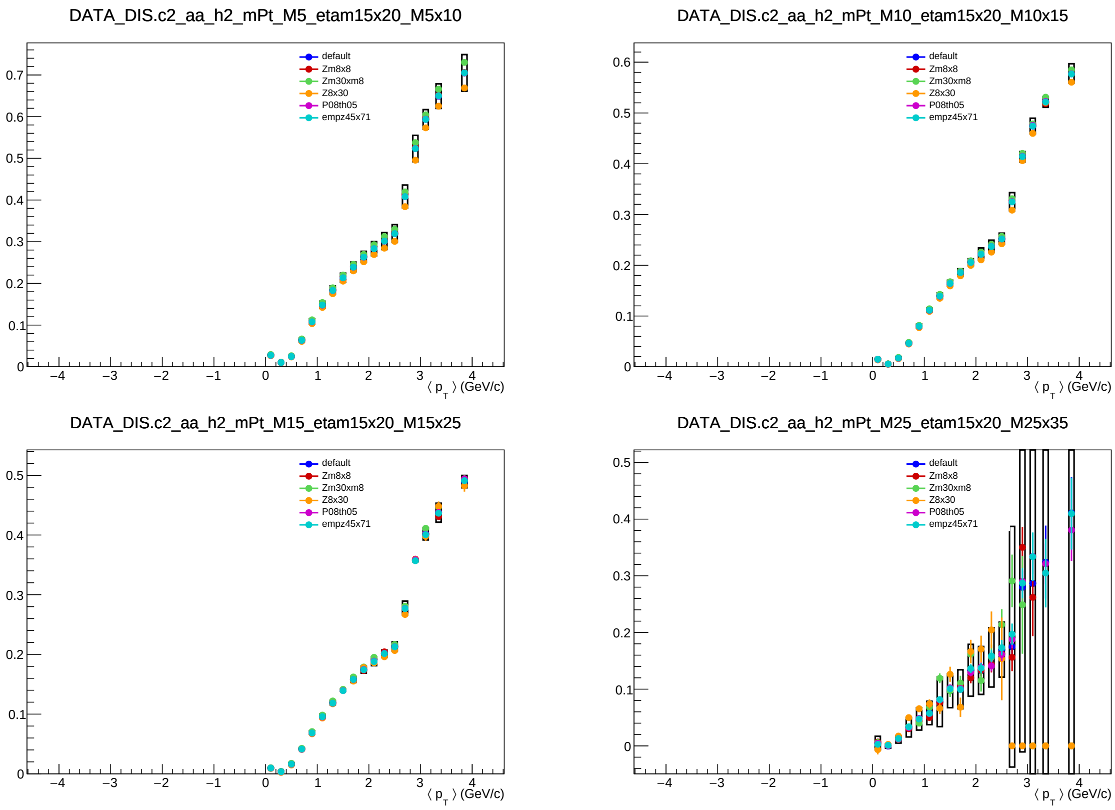

Figure 52: *Contributions to the systematic uncertainty for $n = 2$ for different multiplicities.*

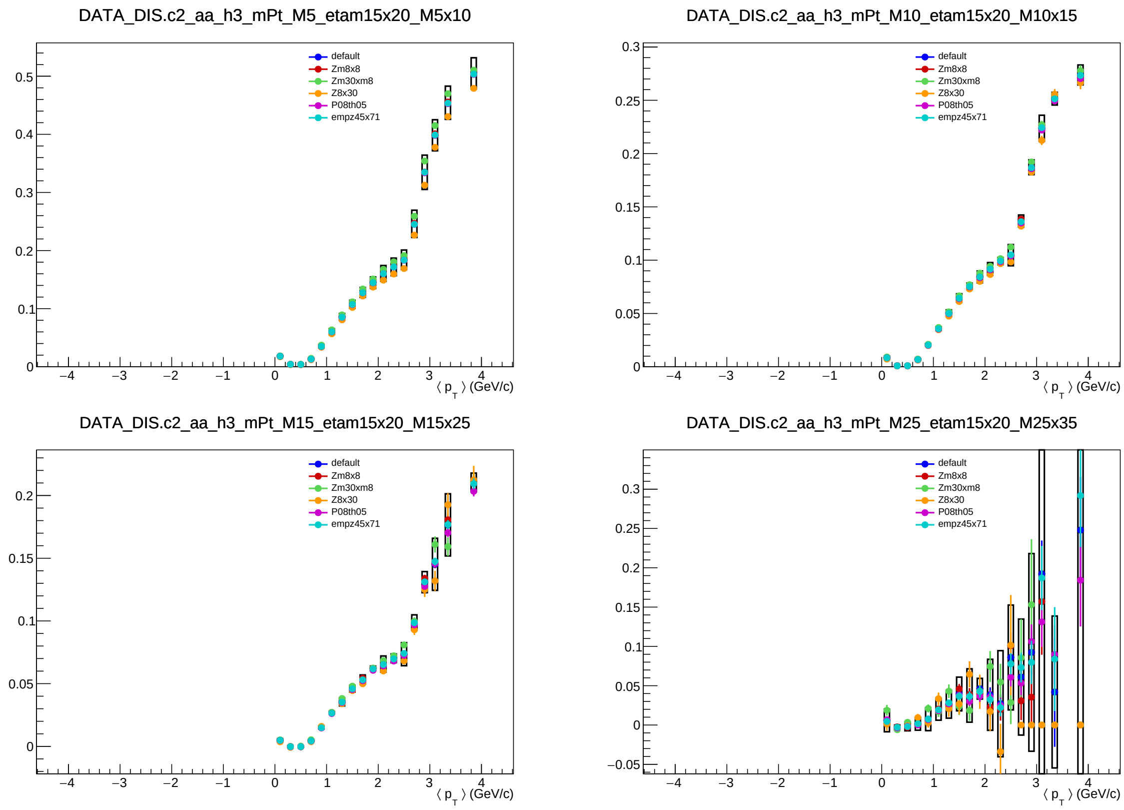

Figure 53: *Contributions to the systematic uncertainty for* $n = 3$ *for different multiplicities.*

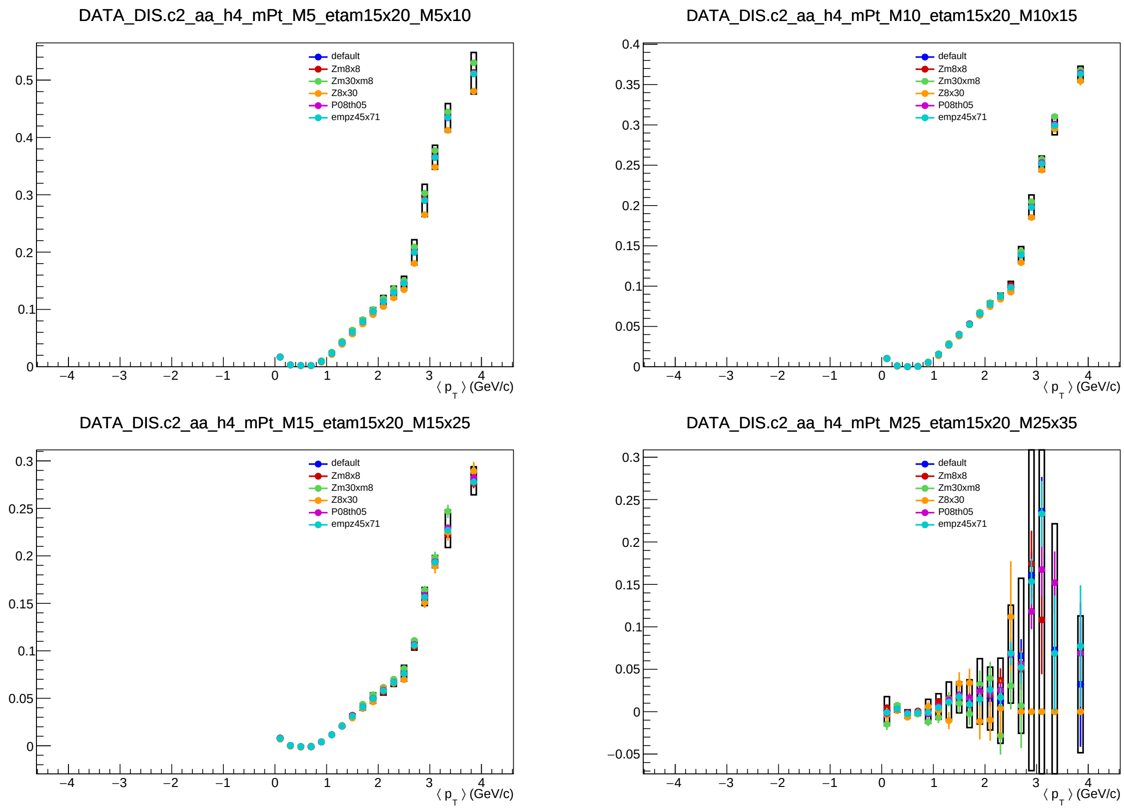

Figure 54: *Contributions to the systematic uncertainty for* $n = 4$ *for different multiplicities.*

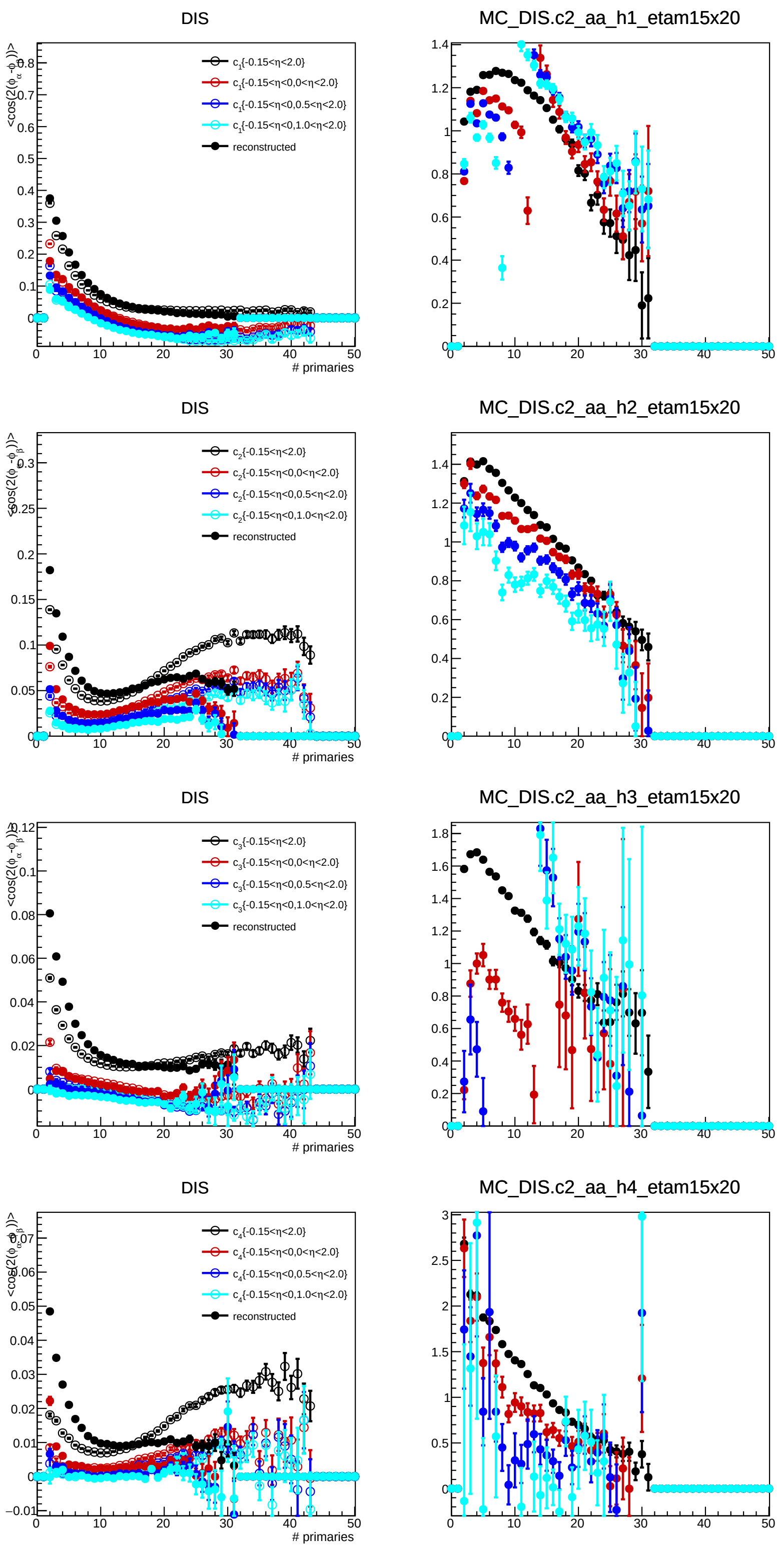

Figure 55: *The measurement of c_2, with generated particles (solid markers) compared to reconstructed particles (open markers). Each figure shows various η-gaps. Clockwise the figures show $n = 1, 2, 3, 4$. to be shown for corrected correlations incl multiplicity*

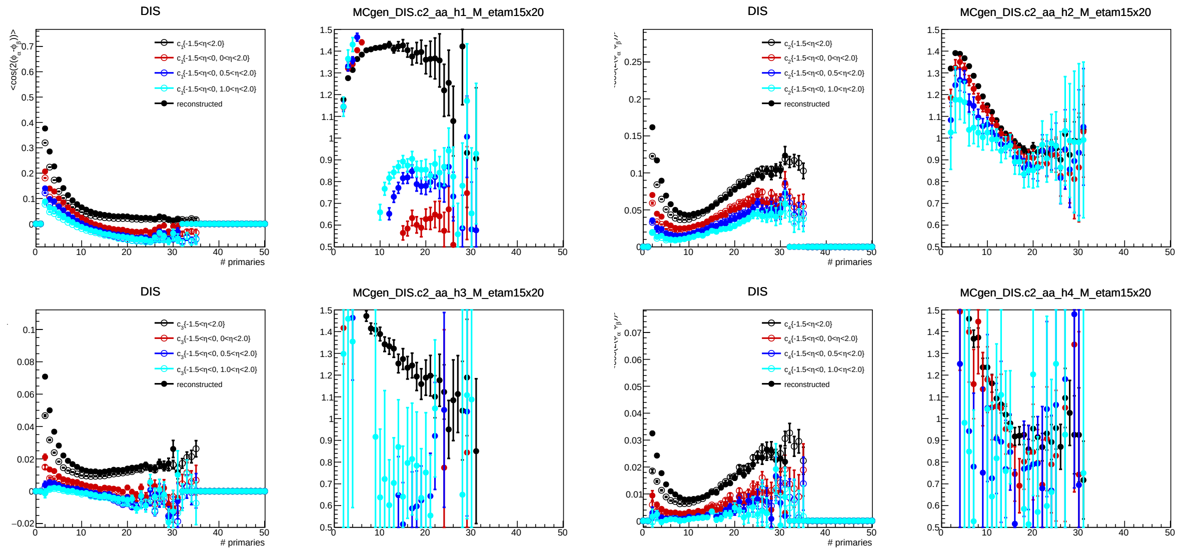

Figure 56: *2-particle correlations versus event multiplicity, left DIS events and right PHP events, and from top to bottom harmonics $n = 1, 2, 3, 4$ for generated particles before and after trigger/event selection.*

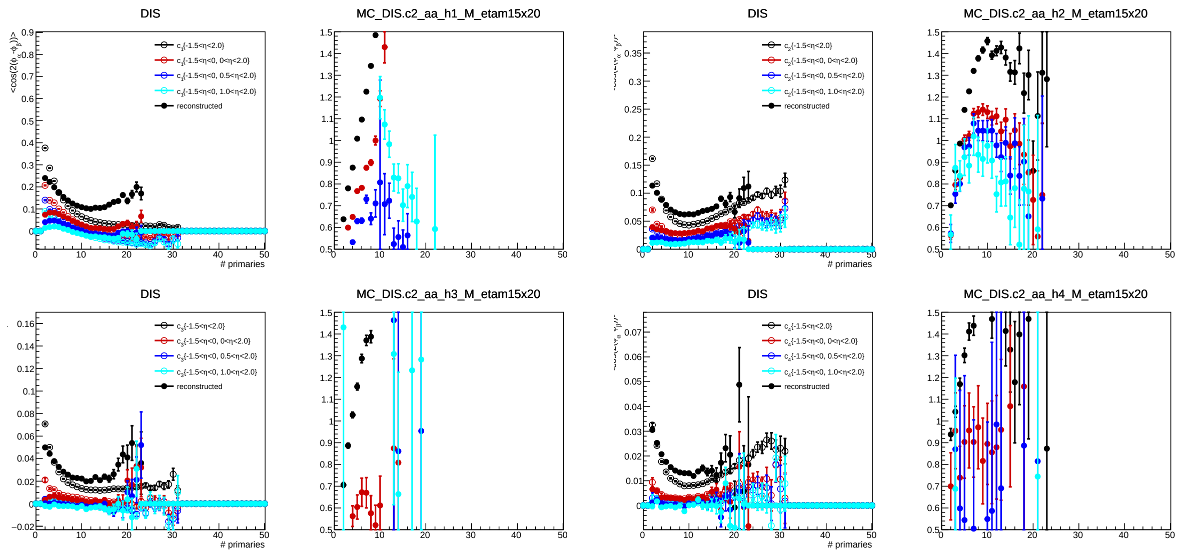

Figure 57: *2-particle correlations versus event multiplicity, left DIS events and right PHP events, and from top to bottom harmonics $n = 1, 2, 3, 4$ for generated and reconstructed particles after event selection.*

9.2 Event selection variation

9.3 Track selection variation

9.4 Tracking efficiency

9.5 Non-uniformity correction

9.6 Monte Carlo closure

9.7 Unfolding

10 Summary

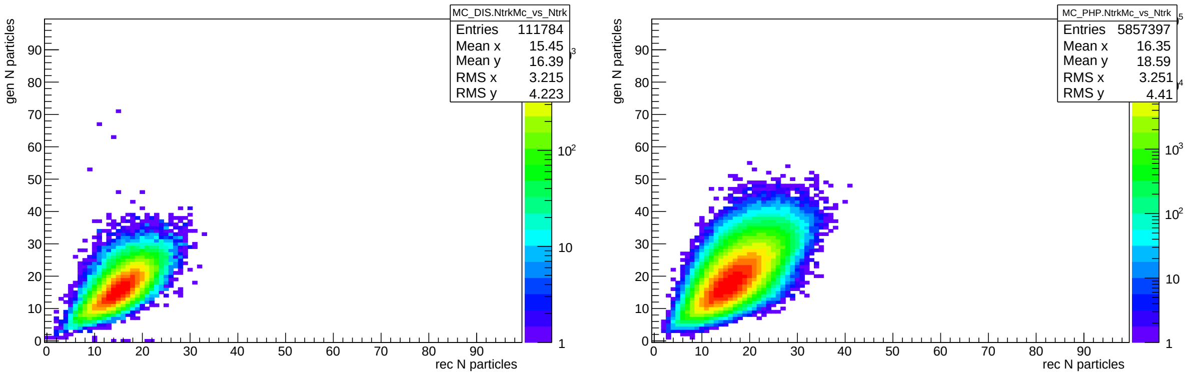

Figure 58: *Unfolding matrices. Left: DIS, Right: PHP*

A Four-particle correlations

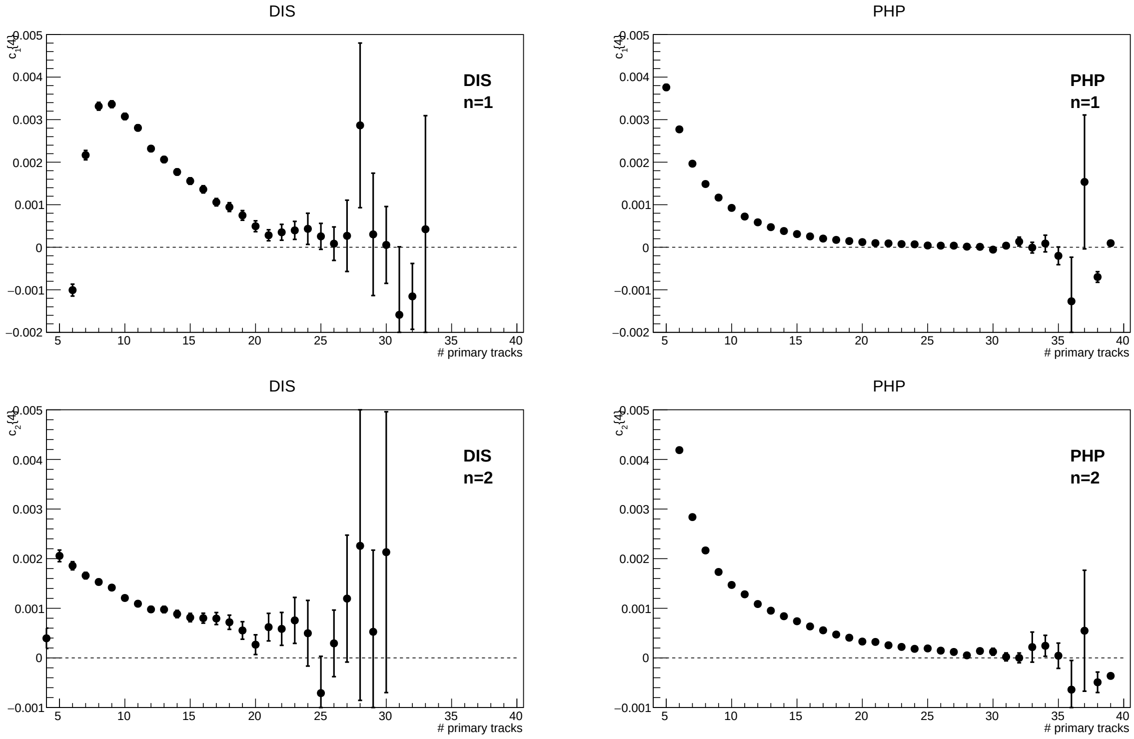

Figure 59: *Four particle correlations*

B $\Delta\eta - \Delta\phi$ 2-particle correlation

C Photoproduction

C.1 Comparisons to data

C.2 PHP

C.3 Comparison of DIS and PHP

Comparison of 2-particle correlation versus event multiplicity with DIS on the left and PHP on the right.

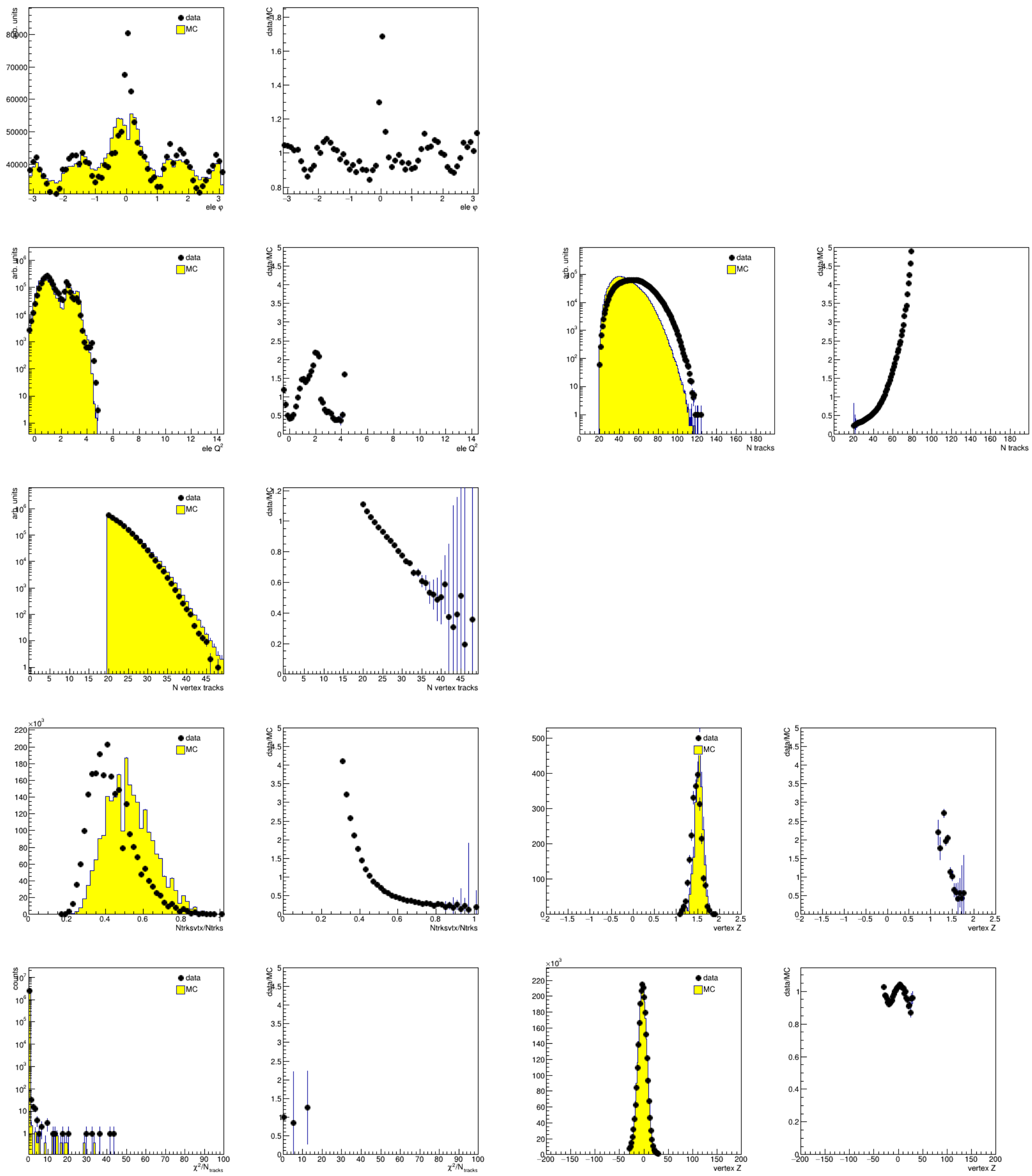

Figure 60: *Event distributions of data and MC. The distributions are for PHP selected events from 06p and ari_incl_nc_PHP_lowQ2_06e. In the first and third column the distribution in MC (yellow) and data (black dots), with to the right of that the ratios of data to MC.*

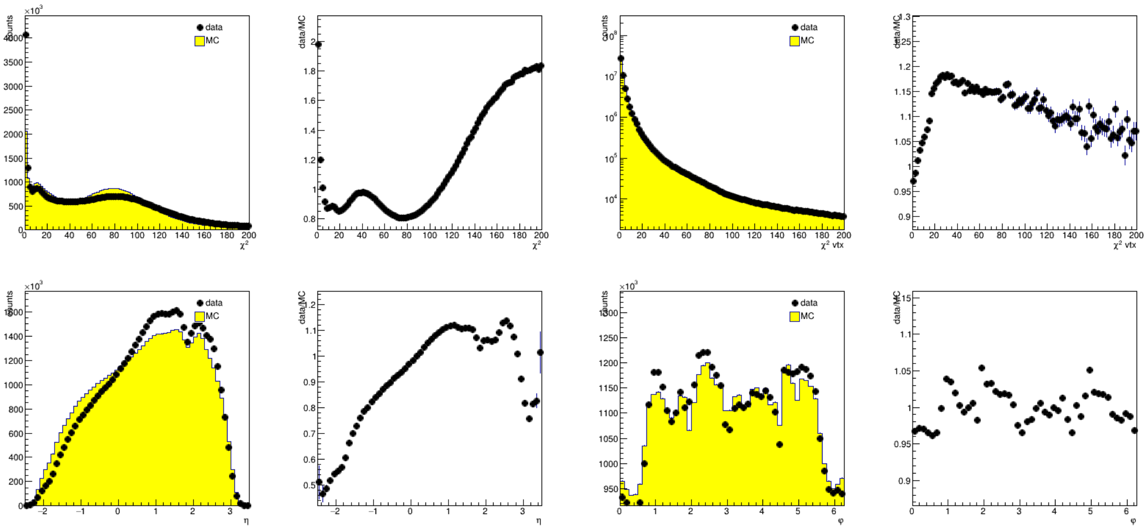

Figure 61: *Track distributions of data and MC. The distributions are for PHP selected events from 06p and ari_incl_nc_PHP_lowQ2_06p. In the first and third column the distribution in MC (yellow) and data (black dots), with to the right of that the ratios of data to MC.*

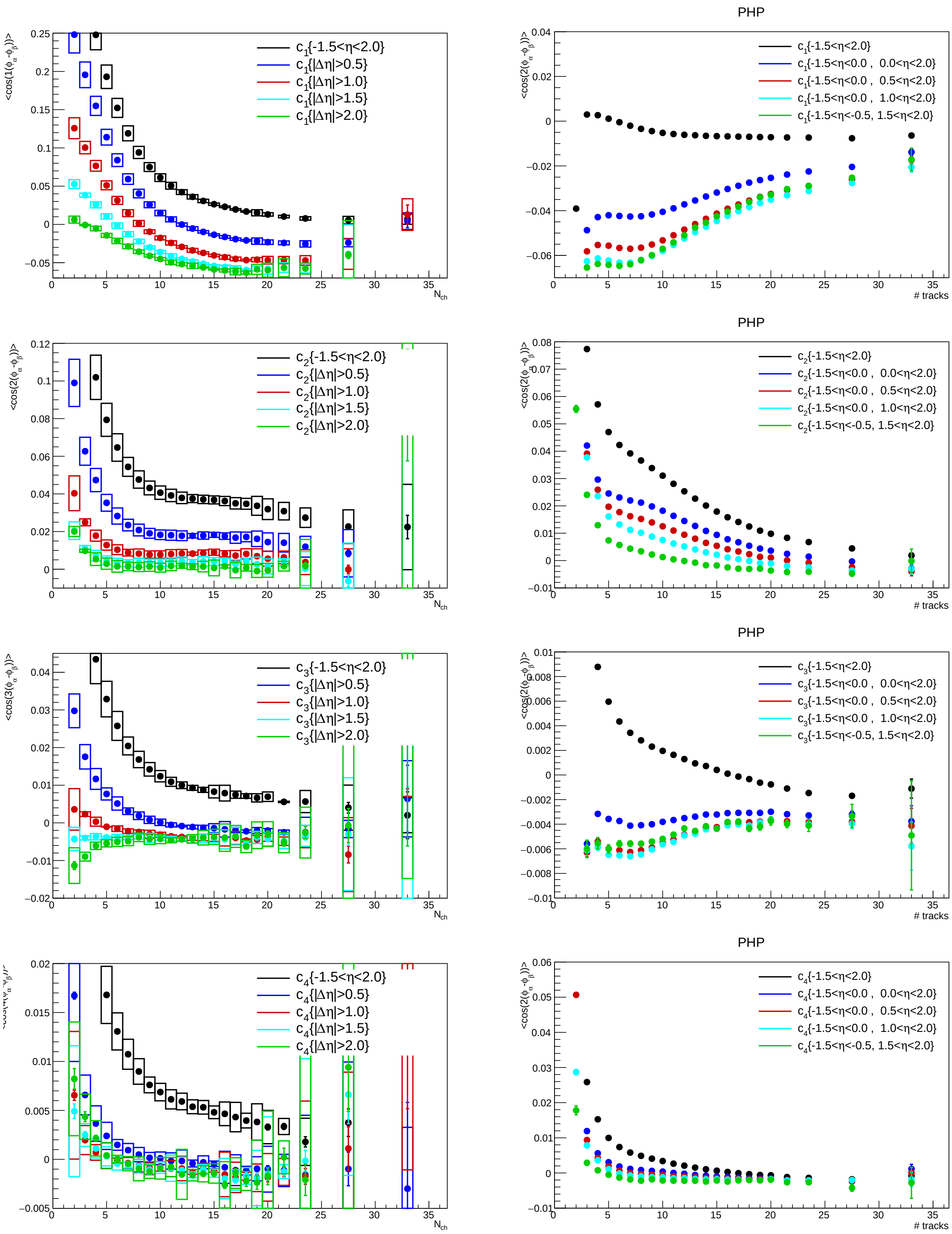

Figure 62: *2-particle correlations versus event multiplicity, left DIS events and right PHP events, and from top to bottom harmonics* $n = 1, 2, 3, 4$.

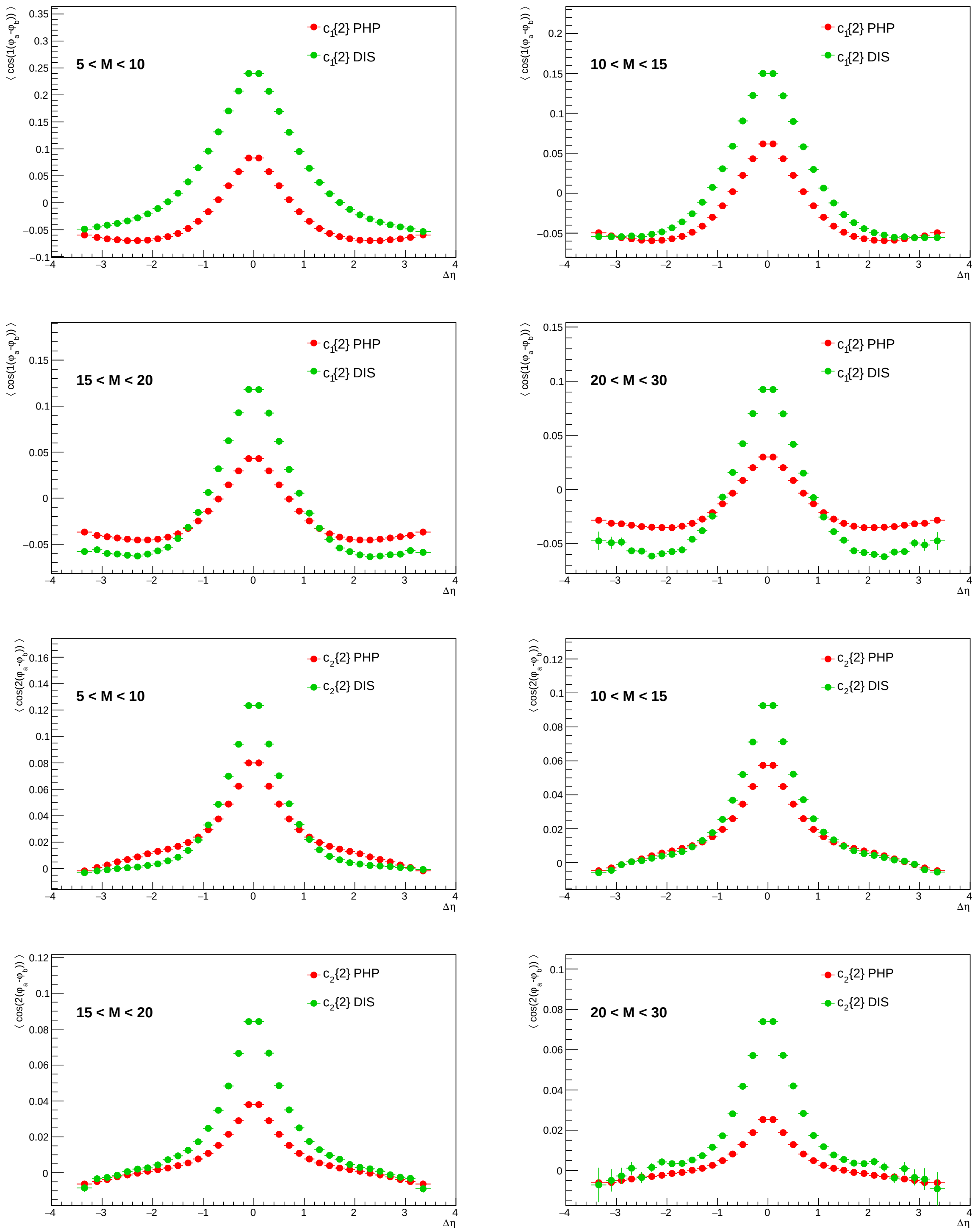

Figure 63: *Differential in* $\Delta\eta$ *for harmonics* $n = 1, 2$*, with varying multiplicity ranges from top to bottom.*

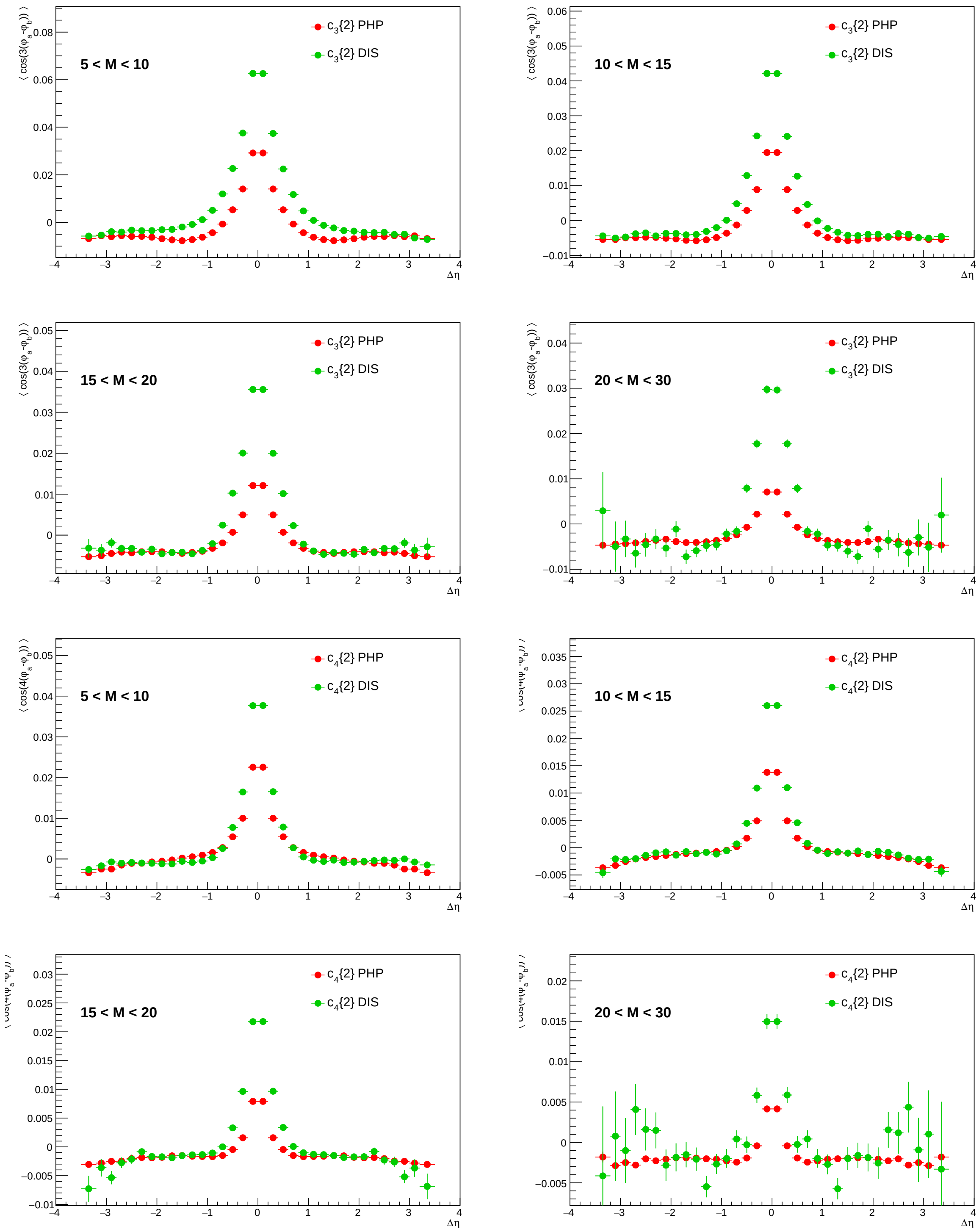

Figure 64: *Differential in $\Delta\eta$ for harmonics $n = 3, 4$, with varying multiplicity ranges from top to bottom.*

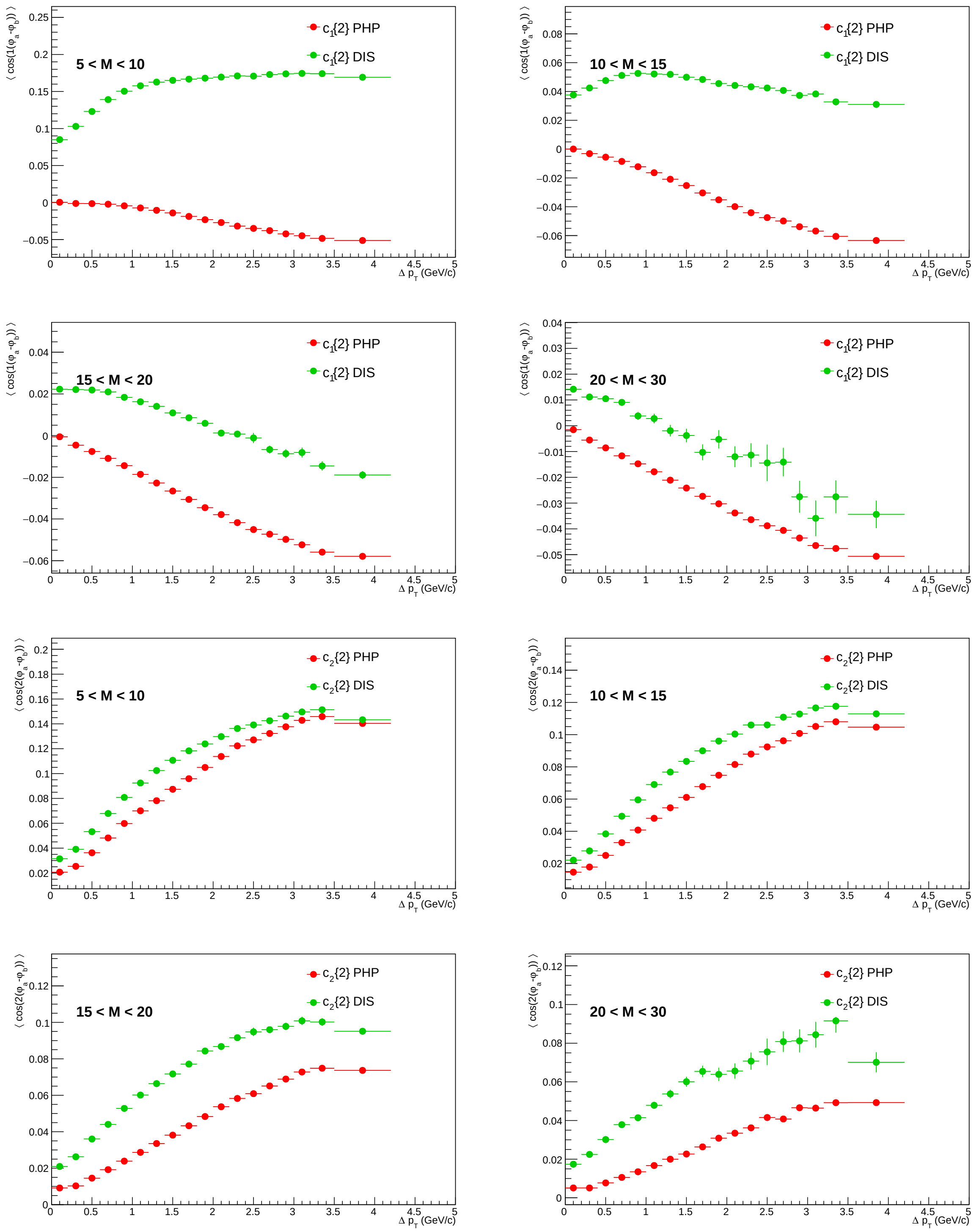

Figure 65: *Differential in* Δp_{T} *for harmonics* $n = 1, 2$, *with varying multiplicity ranges from top to bottom.*

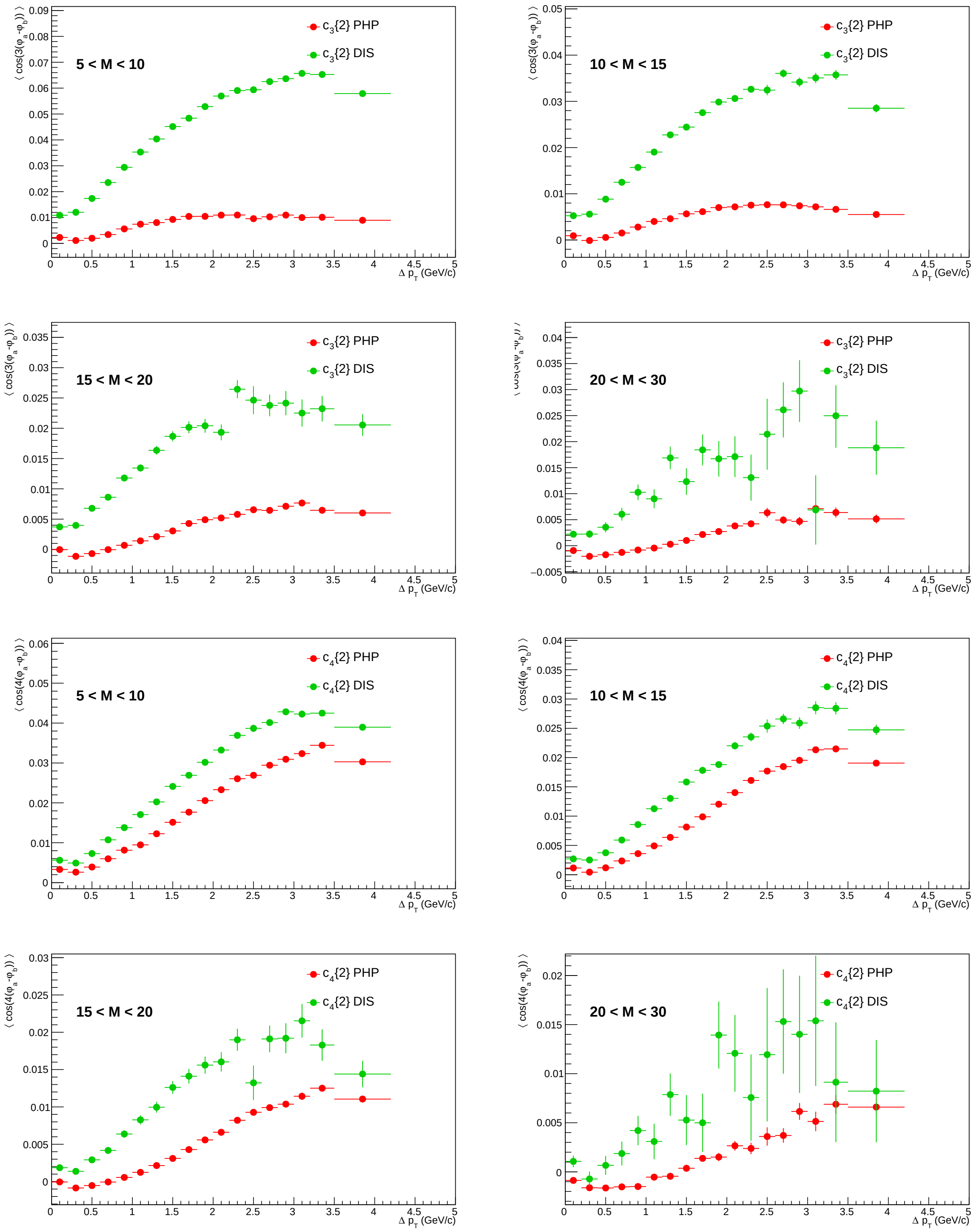

Figure 66: *Differential in* Δp_{T} *for harmonics* $n = 3, 4$*, with varying multiplicity ranges from top to bottom.*

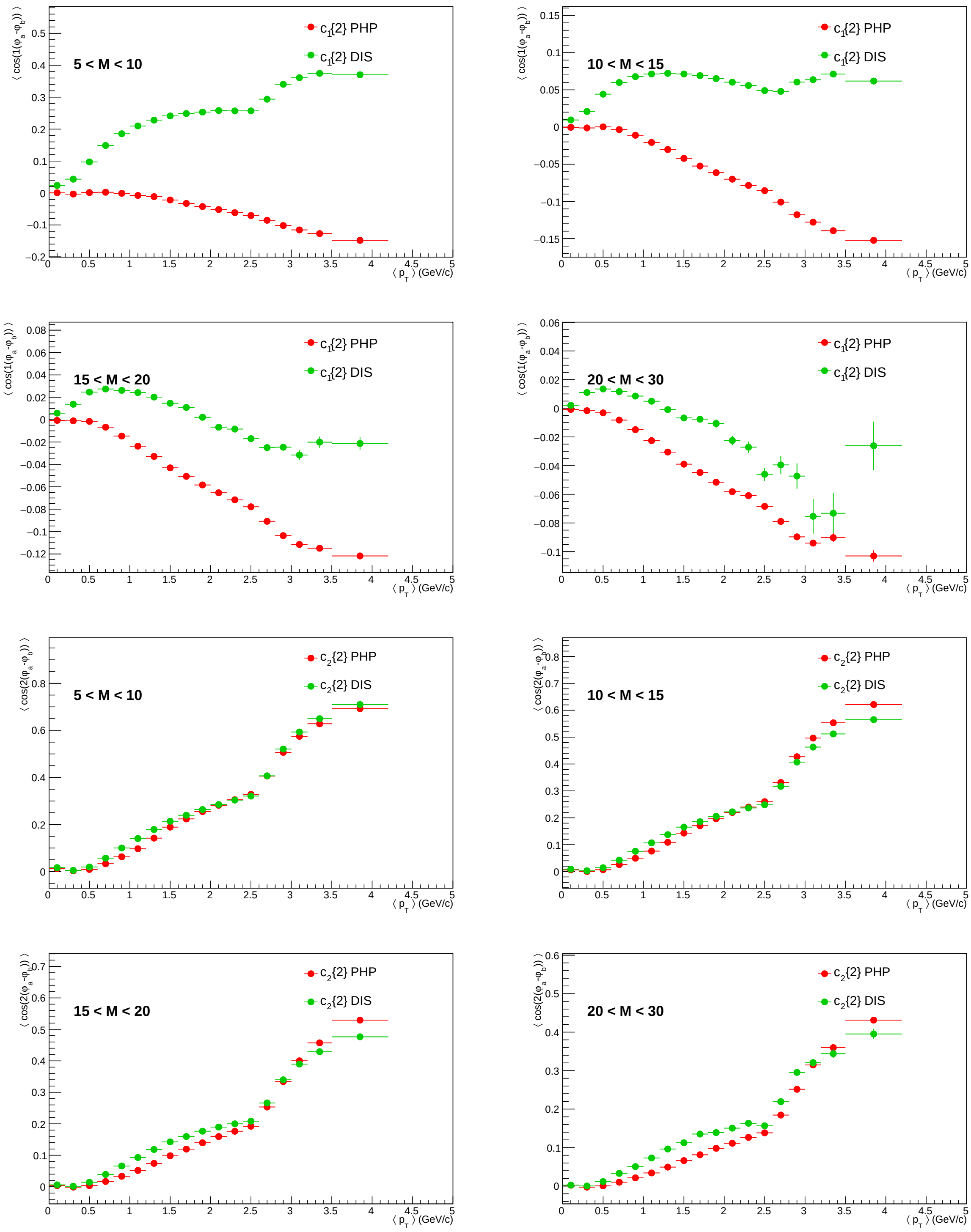

Figure 67: *Differential in* $\langle p_{\mathrm{T}} \rangle$ *for harmonics* $n = 1, 2$*, with varying multiplicity ranges from top to bottom.*

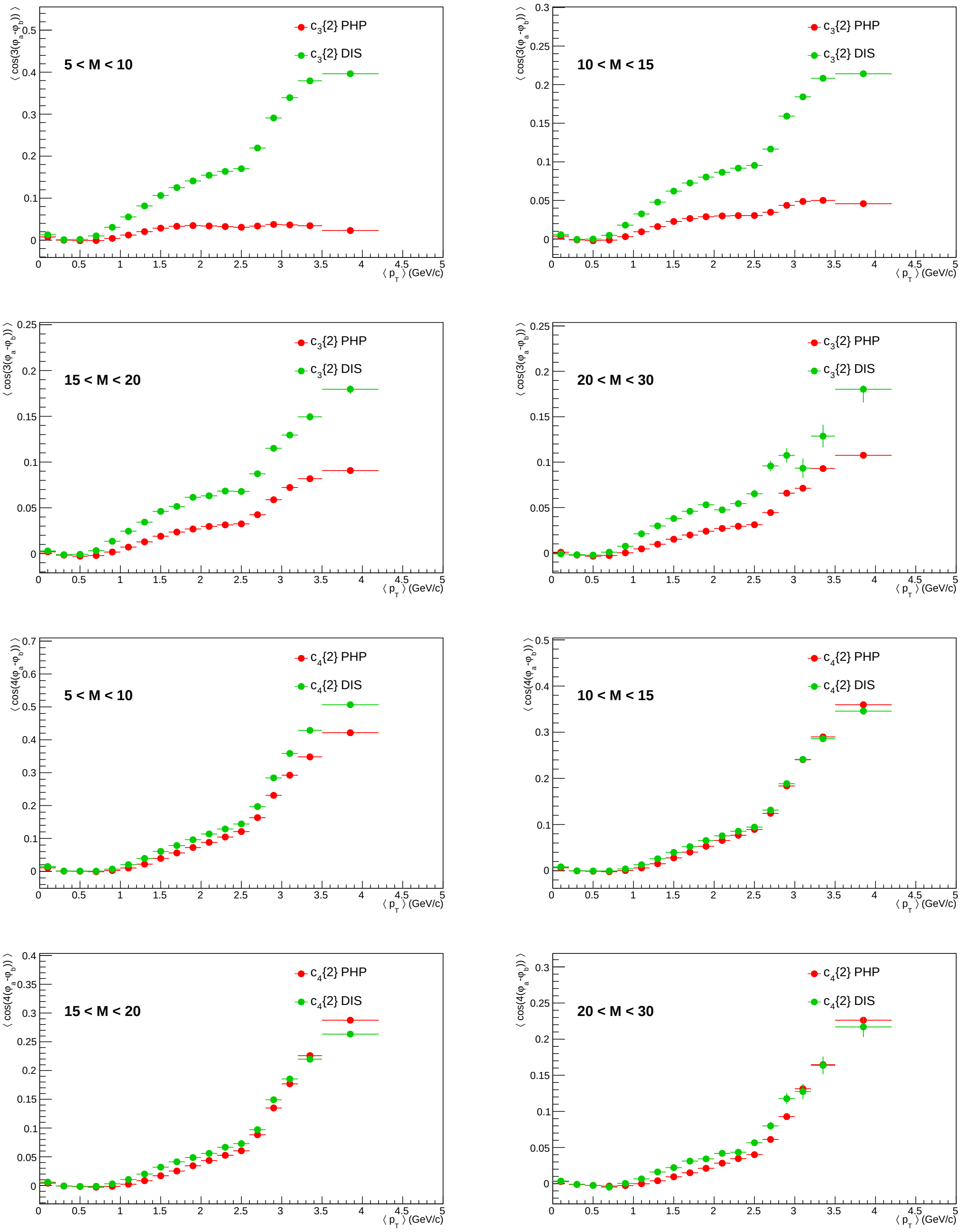

Figure 68: *Differential in* $\langle p_{\mathrm{T}} \rangle$ *for harmonics* $n = 3, 4$*, with varying multiplicity ranges from top to bottom.*

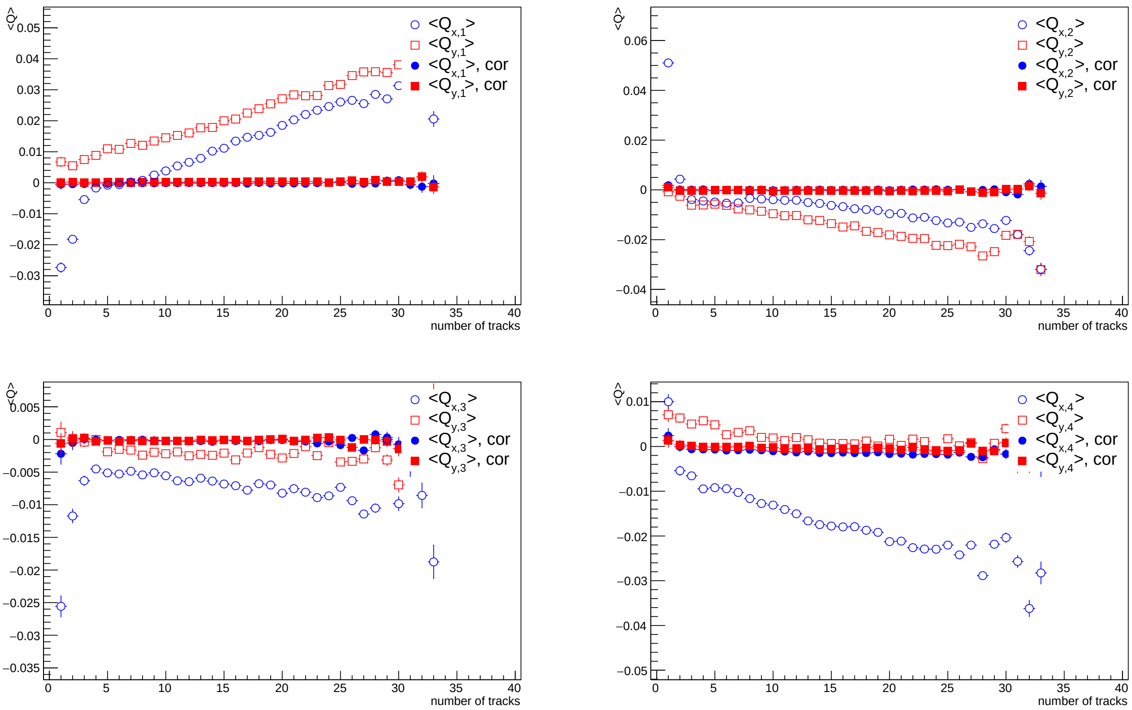

Figure 69: *$\langle Q_{x,y} \rangle$ as a function of event multiplicity for PHP events, showing uncorrected (open symbols) and corrected (full symbols) $\langle Q_{x,y} \rangle$, and clockwise the harmonics $n = 1, 2, 3, 4$.*

C.4 Technical documentation

Git: `https://gitlab.cern.ch/ISOQUANT/ZEUS`

C.4.1 Run analysis

Login to hera pool: ssh nafhh-x1.desy.de
Login to hera cluster: ssh nafhh-zeus01

Analysis code:

- main.c
  Runs the code (compile with build.sh)
- configTask.C
  Configuration of analysis task parameters.
- cumulantAnalysis.C
  Analysis task
- cumulants.h
  Definition of cumulant formulas
- CalHist.cxx
  Contains definition of $\eta - \phi$ histograms for the corrections
- CalHists.cxx
  Contains an instance of $\eta - \phi$ histograms for different event/track classes
- histogramManager.cxx
  Defines event and track class histograms.
- orangeAnalyser.cxx
  MakeClass of the orange trees, only branches used in analysis are activated and orangeAnalyserFriend is added as friend class.
- orangeAnalyserFriend.cxx
  Contains getters for tree variables, as well as functions to define DIS trigger selection, event quality selection, track selection, MC weights and various MC helper functions.
- QCumulants.cxx
  Contains all correlation histograms and fill functions
- QvecSelection.cxx
  Defines the track selection for an instance of a Qvector

- Qvector.cxx
  Qvector components and harmonics
- build.sh
  Compiles the code
- submitJobs.py
  Submits jobs to cluster: python submitJobs.py <number of files per job> <maximum number of jobs>
  Configure the data to be run over, the output folder and files to be copied.
- nafgo2.sh
  Executes the code on the cluster.

After building the code with build.sh, test code with

```
./readTupleexecutable.o <"DATA"/"MC"> <version> <data identifier string>
<GEN trigger> <PHP trigger> <DIS trigger>
<number of files per job> <number of jobs> <output directory>
```

For example:

```
./readTupleexecutable.o "MC" "v08b" "ari_incl_nc_DIS_lowQ2_06e" 0 1 1 14 1 $PWD
```

After running code on the farm, check output with:
python manageJobs.py <timestamp>

C.4.2 Process analysis output

- plot2p.c
  Plots the 2-p correlations